Numerical Modeling of Fire Island Storm Breach Impacts Upon Circulation and Water Quality of Great South Bay, NY

Daniel C. Conley
Marine Sciences Research Center,
State University of New York,
Stony Brook, NY 11794-5000

Final Report to the National Park Service

MARINE SCIENCES RESEARCH CENTER
STATE UNIVERSITY OF NEW YORK

Numerical Modeling of Fire Island Storm Breach Impacts Upon Circulation and Water Quality of Great South Bay, NY

Daniel C. Conley
Marine Sciences Research Center,
State University of New York,
Stony Brook, NY 11794-5000

Final Report to the National Park Service

MSRC Special Report 124
Reference No. 00-01

EXECUTIVE SUMMARY

Recent perceptions of heightened storm activity, barrier island overwashing and barrier island breaching on the south shore of Long Island, NY have generated considerable interest in the prospective impacts of new tidal inlets formed in the barrier islands bordering Great South Bay and Moriches Bay. At the request of the National Park Service, this study was performed in order to attempt to quantify what the physical effects would be if barrier island breaching occurred at several of the more likely sites. The specific impacts studied were, increased flooding potential due to increased tidal transmission, changes in sedimentation and bottom configuration due to altered current and bed stress patterns, alterations of the salinity distribution from new tidal mixing patterns and water quality effects from modified circulation.

A high-resolution two-dimensional depth integrated finite difference circulation model for the transport of momentum and salt was used to investigate these issues. A baseline model bathymetry was developed primarily from digital bathymetry archives. Additional bathymetries with hypothetical inlets were developed by introducing openings to the ocean at the appropriate spots on Fire Island. These openings had the same tidal transmission characteristics of the 1992 Little Pike's Inlet breach on Westhampton Beach Island. The model was successfully tested using sea surface elevations collected in a field component of the project. Model simulations of the distribution of salinity exhibited discrepancy with monitoring data at locations where the true local freshwater input is significantly higher than the distributed pattern used in the simulations as well as at the inappropriately closed western boundary. However, validation performed by simulating the Little Pike's Inlet breach indicated that the model reliably simulated observed changes in salinity even in regions where the absolute salinity levels were poorly predicted.

In addition to the Pike's Inlet simulations, additional breaches on Fire Island were simulated at Old Inlet and Barret Beach. The former site represents a relatively recent historical inlet and the only site on the island presently experiencing cross-island overwash. The latter site is the narrowest part of the island and is representative of sites on the island that have the largest hydrodynamic potential for breaching.

The simulated breach at Old Inlet showed relatively minor change in tidal transmission with an additional 4% of the 1.1 m ocean tide being transmitted to most of Great South Bay. In the immediate vicinity of Old Inlet a similar reduction in tidal transmission is experienced due to the local change in the nature of the tidal potential. The Old Inlet region does experience an increase in strong currents and associated bed stress with a region in which sandy sediments would be expected to predominate extending across much of the width of the bay. It is argued that the shallow section on the bay side of the breach site would tend to act as an impediment to the development of a permanent inlet here. A reduction in the tidal currents emanating from Fire Island Inlet suggests a large region in the center of the bay in which the formerly sandy bottom would be expected to shoal and shift to finer sediments. Significant advection is observed to

develop between the breach and Fire Island Inlet introducing direct net transport of water from the ocean to the bay. This transport traverses formerly stagnant regions of the bay and would no doubt greatly increase water quality.

The simulations indicate that a breach at Old Inlet will raise the mean salinity of the bay from 25.9 ppt to 29.5 ppt. This change is relatively evenly distributed over the entire Great South Bay with the exception of the inlet exit regions where little change is predicted. A global fresh water residence time calculated for this configuration is 39.5 days, a 60% reduction from the 96.3 days computed for the baseline simulation.

The simulated breach at Barret Beach predicts an increase in tidal transmission over all of Great South Bay with the changes ranging from 2-4% of the 1.1 m ocean tide. Bottom shoaling and a fining of the bottom sediments is predicted for a large section of the central bay, similar to that predicted for Old Inlet. The development of new areas of high bed stress only near the inlet suggests little resistance to inlet development in this location. Net transport between Barret Beach and Fire Island Inlet will also lead to improved water quality and reduced residence times although the effects will be more limited to the center of the bay than with Old Inlet.

The mean bay salinity is predicted to increase to 28.7 ppt but the changes are not evenly distributed across the bay. The increase comes from an up to 5 ppt increase in the western two thirds of Great South Bay and is counter balanced by a 1-2 ppt decrease in eastern Great South Bay. While calculated global residence time is reduced to 51.9 days, it is not as low as for Old Inlet reflecting the isolation of eastern Great South Bay.

The field observations and previous work suggest that sub-tidal storm induced circulation may be as important as tidal processes in determining the salinity and water quality of Great South and Moriches Bays. In addition, the effects of breaches on the flooding potential of these effects may in fact be opposite that observed in this study. These effects have not been addressed in this work and should be part of a follow up study. While realistic breach geometry was used for this study, little is known about what the equilibrium size of a breach in Fire Island would be and whether such an inlet would be stable. These issues have been discussed here qualitatively but a more detailed examination of this issue is called for.

Table of Contents

LIST OF FIGURES

LIST OF TABLES

Numerical Modeling of Fire Island Storm Breach Impacts Upon Circulation and Water Quality of Great South Bay, NY

Daniel C. Conley
Marine Sciences Research Center,
State University of New York,
Stony Brook, NY 11794-5000

BACKGROUND

A series of strong extra-tropical storms in the early 1990's led to severe dune erosion and apparent shoreline recession on much of the southern shore of Long Island, NY. Reduced barrier cross-sectional area from these storms eventually culminated in the multiple breaching of the barrier island at Westhampton Beach in early December of 1992 (Figure 1). The eventual enlargement of one of these breaches (Little Pike's Inlet) led to wide spread speculation about the possible impacts of such a breach. Concerns ranged from heightened flooding potential, detrimental changes in water circulation and altered water quality leading to undesirable shifts in estuarine species composition. This study was designed to begin to address these concerns by providing quantitative predictions regarding the physical changes which could be expected to arise from barrier breaching at various locations in the Great South Bay-Moriches Bay system.

In shallow estuarine systems where local tidal forcing is negligible, the majority of fluctuations in the water surface elevation occur as a response to the imbalance between the water level inside the estuary and the tidally modulated coastal sea surface elevation adjacent to the estuary. Thus, the sea level fluctuations inside the bay (hereafter referred to as the "bay tides") can be considered to be forced by the coastal tidal signal. This forcing leads to a physical exchange of water through the connection between the estuary and the ocean, namely, the inlets. Some fraction of this forcing is dissipated, largely through frictional effects in the inlets, so that the bay tides are typically neither as great as, nor synchronous with, the coastal tides. As a result, inlets can be conceived as filters that do not pass the forcing in its entirety, but in general change the amplitude and introduce phase shifts which are dependent on the frequency of the forcing. The magnitude of these changes is dependent on such parameters as inlet cross section, length, bottom roughness and characteristics of the approaches to the inlet [Mehta and Joshi, 1988; van de Kreeke, 1988; DiLorenzo, 1988; Keulegan, 1967]. Alterations of these parameters as well as additions or reductions in the number of inlets in a system can result in significant adjustments in the net filter characteristics of the system.

Commonly, the circulation in such systems is either totally or predominantly driven by this associated ocean-estuary exchange, so that inlet changes can be seen not only in altered "tidal" ranges but also in the patterns and strength of circulation. In systems where fresh water input is present, estuarine salinity is reduced relative to that in the nearby ocean. This reduction represents a balance between the fresh water input and the exchange with the saline ocean. Any alteration of this exchange shifts this balance resulting in a different salinity for the bay system. In larger systems, where salinity is not uniform throughout the bay, alterations of the patterns of circulation may result in changes of local salinity within the estuary even if the overall spatial mean is unchanged. It is reasonable to assume that other quantities such as water temperature, or dissolved oxygen or pollutant concentrations, which exhibit different distributions between the estuary and the coastal ocean, may also be affected by inlet alterations.

Many studies have reported on the effects of inlet changes on the physical and biological properties of estuarine or back bay systems. A commonly reported example pertains to the

barrier at Chatham, Ma [Giese, 1988]. This barrier appears to go through a cyclical process of buildup and extension, breaching, erosion and onshore migration followed by the reinitiation of buildup. Following the most recent breaching of the barrier at the entrance to Chatham Harbor, Giese [1988] reported a tidal range of 1.4m which represents a 30% increase when contrasted to the pre-breach range of 1.1m. Human intervention in inlet systems has also been seen to lead to significant changes in lagoonal circulation and characteristics. Following the construction of a pass from the Gulf of Mexico into a branch of Galveston Bay, Reid [1957] observed a complete reversal of the spatial gradient of salinity in the bay that was associated with the doubling of salinity values in some regions of the bay. This physical change was accompanied by significant biological adjustment in which the dominant species of fin fish were observed to shift throughout the bay.

Fire Island and the other barrier islands on the south shore of Long Island (Figure 1) have experienced repeated breaching [Leatherman, 1989] and the effects of several recent episodes have been documented. Turner [1983] observed slow growth in the hard clam population in Moriches Bay for the year following the 1981 breach at Moriches Inlet. Monitoring of Moriches Bay following the Little Pike's Inlet breach indicated an increase in the tidal range in part of Moriches Bay of over 30% relative to a pre-breach range of 0.76 m [Conley, 1999]. A concurrent 1.3 ppt increase in salinity was observed in the eastern portion of the bay nearest the breach although no salinity change was observed in the western section of the bay near the connection with Great South Bay.

It is clear that there are discernible effects associated with barrier island breaches and that many of these effects have societal repercussions. As much of the Fire Island National Seashore (FINS) is protected wilderness area, the preparation for and response to such an event must be based on a balance between the impact of the effects and the mandate of the National Park Service (NPS) as custodian of the Seashore. In order to determine the appropriate response, the NPS asked for an assessment of the potential impacts of possible future breaches within the domain of FINS. This report describes the results of a numerical modeling effort designed to make such predictions.

This study uses a full numerical model of the Great South Bay with present and hypothesized inlets to understand the expected effects of new breaches and inlets on the bay. The specific questions to be answered are: how would tidal transmission vary with different inlets; how would the distribution of salt vary with the formation of these new inlets; what would be the mean and instantaneous circulation patterns with these new geometries and how stable would the new and pre-existing inlets be? This information will provide Seashore managers with a relatively complete set of hydrodynamic information upon which to base any decision on how to respond to barrier island breaching.

MODEL DESCRIPTION

The most basic approach to such a project would be the application of a simple inlet basin model in which each basin and inlet are parameterized with respect to their storage and transmission characteristics and then these individual units are linked together to study their interactions with each other. While computationally very inexpensive, this type of study was rejected as the results would represent a basin wide average and provide no information about localized effects within each basin. Full numerical simulation of estuaries is commonly performed using finite element schemes which permit adjustment of the grid size so that finer detail can be obtained at narrow constrictions such as inlets and coarser grid sizes can be used in larger more homogenous regions such as basin interiors. This approach saves on computational resources but the simulation of new inlets in such a process would require the development of

new computational grids for each new case. As validation for these hypothetical cases is clearly not available, it was decided to use a finite difference numerical model in which the numerical grid would remain fixed for all the simulations performed and validation performed on the original model could be assumed valid for the subsequent simulations.

The model used for this work is a 2-D, depth integrated, non-linear, finite difference model for the transport of momentum and salt. The model is derived from the external modes of the SWK3D 3-dimensional model described in Koutitonsky et al [1987] which was originally designed for use in semi enclosed bodies of water. The model has since been applied to, and validated in, other coastal and shallow water environments in several studies [e.g. Valle-Levinson and Wilson, 1994; Chant, 1995; Ullman and Wilson, 1998]. The hydrodynamic model includes baroclinic pressure gradients, Coriolis terms, linear and non-linear accelerations and quadratic bottom stress through the application of a bottom friction factor C_f.. Horizontal mixing is modeled using a diffusive mixing parameter (A_H). Salt transport includes both advection and horizontal mixing through the use of a horizontal mixing coefficient for salt (A_S). The numerical scheme utilizes a C grid for spatial computations with a mixed leapfrog technique for the inertial terms and forward time scheme for the diffusive and dissipative terms. Stability conditions for the model require that the time step has to be small in relation to the time necessary for a linear gravity wave to traverse a grid cell. The model solves the vertically averaged equations for momentum and salt flux at each grid point and then applies the continuity equation to determine local changes in sea surface elevation.

The model required several modifications for the present application. The primary modification was the introduction of a wetting and drying scheme enabling the model to operate in a shallow environment such as Great South Bay. This enhancement of the model was achieved by determining a limiting depth below which the surface elevation in any cell was prevented from going. Operationally, this was achieved by testing newly calculated elevations at each time step to see if they were below the limit depth. When such a situation was encountered, the transport out of the cell was reduced proportionally so that the recalculated depth was equal to the limit depth. Transport out of the cell was then prohibited until transport into the cell had raised the surface elevation above the limit depth. This scheme preserves mass and salt conservation in the model. The limiting depth in all the present simulations was 2 cm. It should be noted that without this modification, the model could not function in this shallow environment with such a small grid-size.

The next major modification involved the development of the freshwater source in the model. Approximately 40 streams and small rivers empty into the north edge of Great South Bay and several more empty into Moriches Bay. However a large fraction of the freshwater input is delivered to the bay as relatively homogenous groundwater seepage with estimates of the seepage contribution ranging from 35% [Pritchard and Gomez-Reyes, 1986] to 95% [Redfield, 1952] of the total freshwater input. It was therefore decided to treat the freshwater input as a line source equally distributed along the north shore of Great South Bay and Moriches Bay. The total 13.79 m^3/s [Pritchard and Gomez-Reyes, 1986] freshwater input into Great South Bay was distributed among the next to the most northerly cell in each of the 286 columns of cells spanning Great South Bay. The penultimate cell was chosen to avoid cells which may be regularly turning on and off due to wetting and drying. An additional 0.69 m^3/s was distributed among 12 northern cells of Moriches Bay to represent the freshwater input to that bay [Redfield, 1952]. These inputs represent a fluid mass input as well as a source of salt dilution so that model computations in these cells had to by altered in order to conserve mass and salt. No freshwater was injected along the narrows at Smith Point.

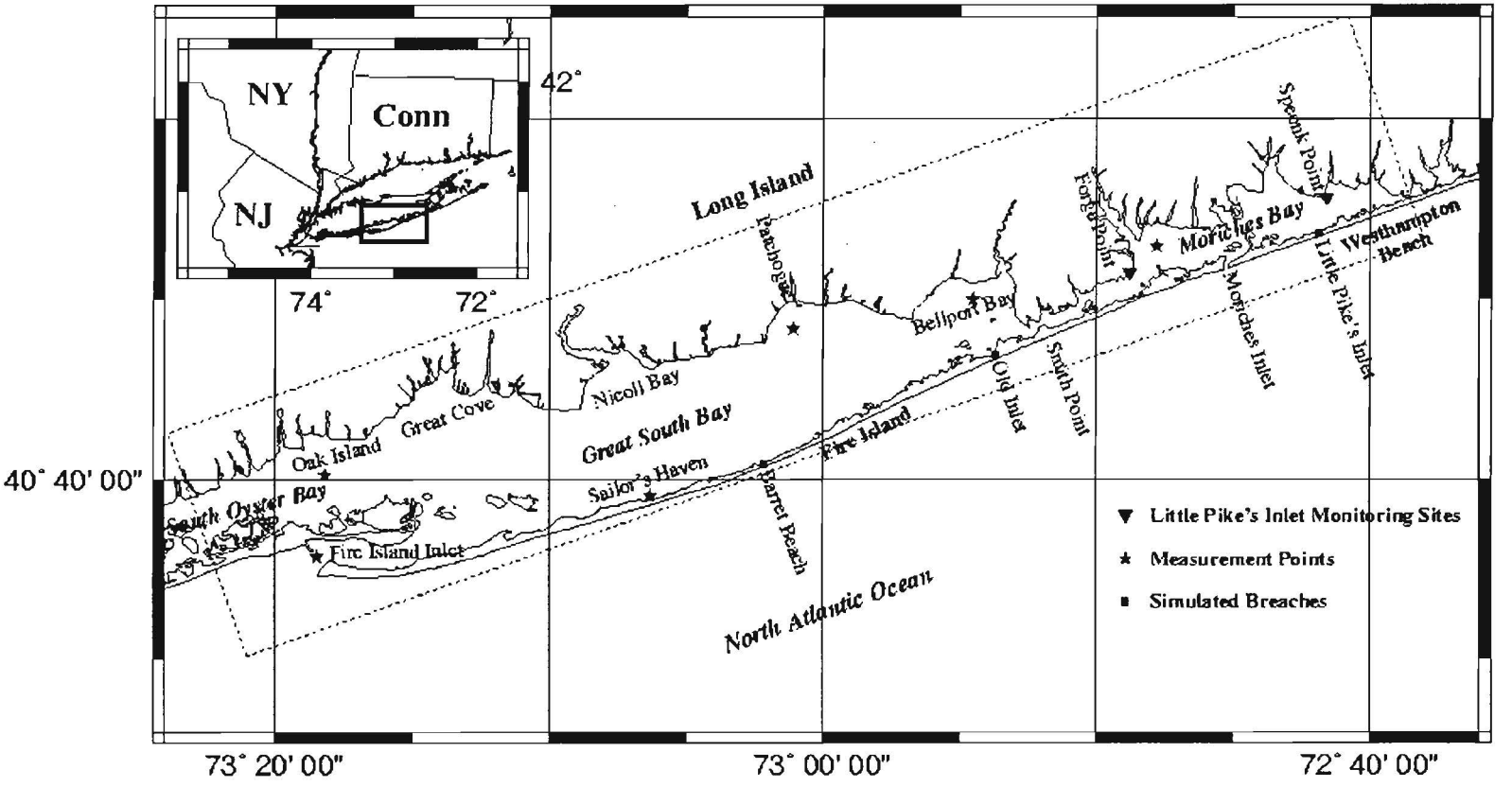

Figure 1 Map of study area. Model domain is indicated by dashed line. Stars denote field measurement sites and triangles indicate Little Pike's Inlet monitoring sites. Small boxes mark the location of the simulated breaches.

Model Bathymetry and Boundaries

In order to fully simulate all the mixing processes which affect the salt balance in Great South Bay, a model domain which covered the entire inter-linked estuarine system of the south shore of Long Island, as well as enough of the New York Bight to adequately simulate plume dynamics would be required. In developing the bathymetry grid for this application, it was recognized that this was beyond the scope of the project. The seaward extent of the model domain was therefore selected as the various inlet mouths at which the coastal tidal elevation forcing would be applied. Elsewhere, the north boundary was composed of the south shore of Long Island and the southern edge of the domain was the north shore of Fire Island as well as pieces of Westhampton Beach Island and Jones Beach Island. The eastern limit to the model was the very narrow (75 m^2 total cross-sectional area) opening into the Quantuck canal. The western limit was the most problematic and was taken to be a relatively shallow cross-section adjoining South Oyster Bay. Earlier models of estuarine circulation in this area [Pritchard and Gomez-Reyes, 1986; Wilson et. al., 1991] indicated that this was a region with small spatial gradients of currents and salinity. In order to maintain a balance between computational requirements and model effectiveness, the grid spacing was selected to be as large as possible while maintaining a minimum of 2 grid points in the narrowest constrictions in the model domain. This criterion resulted in a bathymetry grid spacing of 150 m. Given these restraints, a total grid of 82 (12.15 km) by 430 (64.35 km) cells was required.

The model bathymetry (Figure 2) was determined from 3 different sources. The first source was the NOS digital hydrographic survey database. All bathymetric surveys for this region were collected with individual surveys spanning the period 1933 to 1975. These surveys provided heavy coverage of eastern South Oyster Bay, central and western Great South Bay as well as Fire Island Inlet and associated channels, and far eastern Great South Bay. Notable gaps remained in central and western Great South Bay as well as all of Moriches Bay. The bathymetry in these regions was obtained by digitizing the appropriate areas of NOAA nautical chart12352 (1994) for Great South Bay and Moriches Bay. Terrestrial topography was obtained from USGS 1:250,000 scale Digital Elevation Model files for Nassau and Suffolk counties as well as hand digitized 1:40,000 scale topographic maps where necessary. This collection of randomly spaced bathymetric data was mapped onto the model grid in a 3 step process utilizing the Generic Mapping Tools (GMT) [Wessel and Smith, 1995; Wessel and Smith, 1991]. First, all randomly spaced data was block averaged to provide equally spaced data at 1 arc second spacing. Next, complete coverage of the study area was obtained by applying a simple surface fitting algorithm at 2 arc-second spacing. The depths at the required positions in the model grid were then obtained from simple interpolation of this fine scale gridded data. In a few isolated cases, small scale editing of the data was necessary. Particular effort was required through the narrows at Smith Point, in an area near Heckshire State Park in the northwest corner of the grid that was inappropriately identified as sub-aqueous, and in the entrances to Fire Island and Moriches Inlets. In all cases, fine scale editing was done using NOAA chart 12352 as the bathymetric reference.

The open boundaries at the eastern and western edges of the model were treated as solid boundaries with no flow between them. In the case of the Quantuck canal, this is clearly a reasonable approximation as transport through this narrow passage is minimal. It is less obvious that this is an appropriate approximation at the western end of the grid although the previously discussed results from earlier models suggest that it is a reasonable treatment. A series of tests were run with a radiation boundary condition at this western boundary to see how the results were affected by this treatment. These tests, which were performed for elevation simulations only indicated that such a boundary condition changed the tidal transmission in the western section of the bay by less than 1%. No affect was observed in the central and eastern sections of

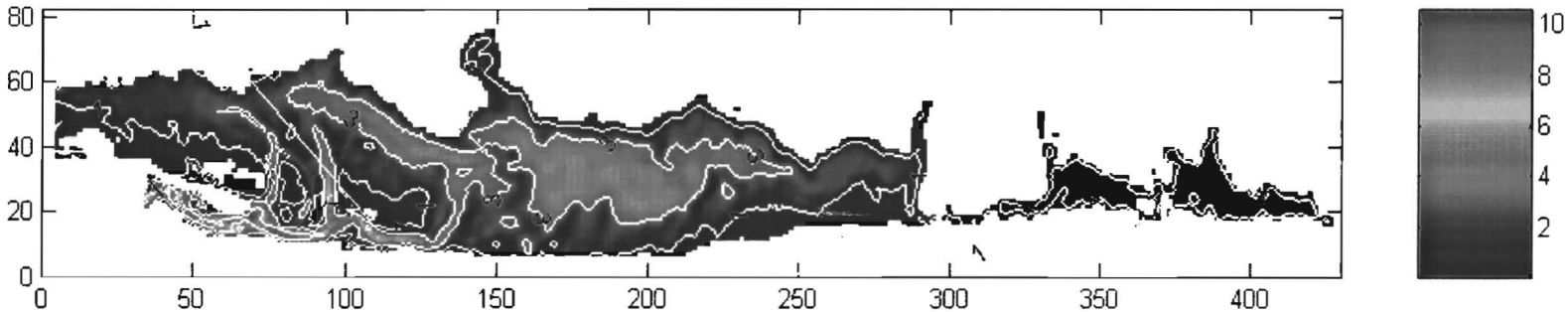

Figure 2 Model bathymetry. Color is representative of the depth at each location. The color bar to right provides the scale in meters. Horizontal and vertical scales are in units of model grid points with 150 m spacing between grid points.

the bay. The only open boundaries in the model are at the inlet mouths where the model is forced with sea surface elevations and velocities are unspecified.

The open boundary conditions for the salinity model are not as straightforward. Even if perfect knowledge of the ocean salinity existed, the water entering the inlet on flood tide is typically a time varying mixture of estuarine water which exited the inlet on the previous ebb tide and oceanic water with which it has mixed. In the absence of a model that includes the full coastal ocean encompassing the entire plume mixing region, some type of parameterization must be developed to adequately describe this process. The scheme used here is the same as that developed by Pritchard and Gomes-Reyes [1986]. The model determines ebb tide salinity normally and then on reversal to flood, salinity at the inlet mouths is linearly increased up to a constant ocean salinity. Once the boundary salinity equals the ocean salinity, it stays fixed at that level until the next ebb tide causes it to decrease again. In the present model, the time required to arrive at the ocean salinity is a constant, known as the "matching time", and represents the final tunable parameter of the model.

The tidal exchange coefficient is a parameter designed to represent what fraction of the flood tidal volume is composed of pure ocean water (as opposed to recycled ebb plume water) [Fischer et al., 1979]. For these simulations, we calculated the effective tidal exchange coefficient from model output and used that information to determine the appropriate inlet matching time. In a study of tidal exchange related to Little Pike's Inlet [Conley, 1999], it was observed that the exchange ratio for Moriches Inlet was approximately 0.18. Observations from that study also suggested that the exchange ratio decreased with the volume of the tidal exchange. With the final Moriches Inlet matching time of 5.5 hours, the exchange ratio calculated from model output was 0.17. As no information was available for the exchange ratio at Fire Island Inlet, a matching time of 4.5 hours was chosen, resulting in an exchange ratio of 0.13 which, considering the order of magnitude greater tidal exchange through this inlet, is qualitatively in line with the above cited principle. These matching times were used throughout the project with the simulated breaches also having a matching time of 5.5 hours.

Field Measurements and Model Testing and Verification

As this model has been extensively used in multiple applications [e.g. Valle-Levinson and Wilson, 1994; Chant, 1995; Ullman and Wilson, 1998], testing in this study related only to the specific application. This consisted of forcing the model with real tide data and then comparing the model predictions of sea surface elevation against observed values at several locations within the model domain. Existing NOAA mean tidal properties were not considered adequate for the present work as they do not provide detailed temporal information of the tidal response to a wide range of forcing conditions. In recognition of this, a field component to the project was carried out with the aid of NPS personnel at FINS. Data for model calibration and validation were collected utilizing a set of six self recording bottom mounted Pressure Temperature, and Conductivity Loggers (PTLC) which were provided by the NPS. These instruments were deployed at six locations (Figure 1) in two consecutive deployment periods which together spanned a 41 day period from 15 March 1995 - 25 April 1995. Data collection was performed in early spring in an attempt to obtain data during a significant storm event. The sensor locations were chosen to sample in separate basins of the model domain as well as to collect boundary information. The collected sea surface elevation and salinity data are presented in Figures 3 and 4 respectively. The total water depth at Fire Island Inlet exceeded the depth range for these sensors so that no elevation data was collected there. Salinity sensors failed at Bellport Bay and Fire Island Inlet during the first deployment and at Fire Island Inlet, Patchogue and Moriches Bay during the second deployment.

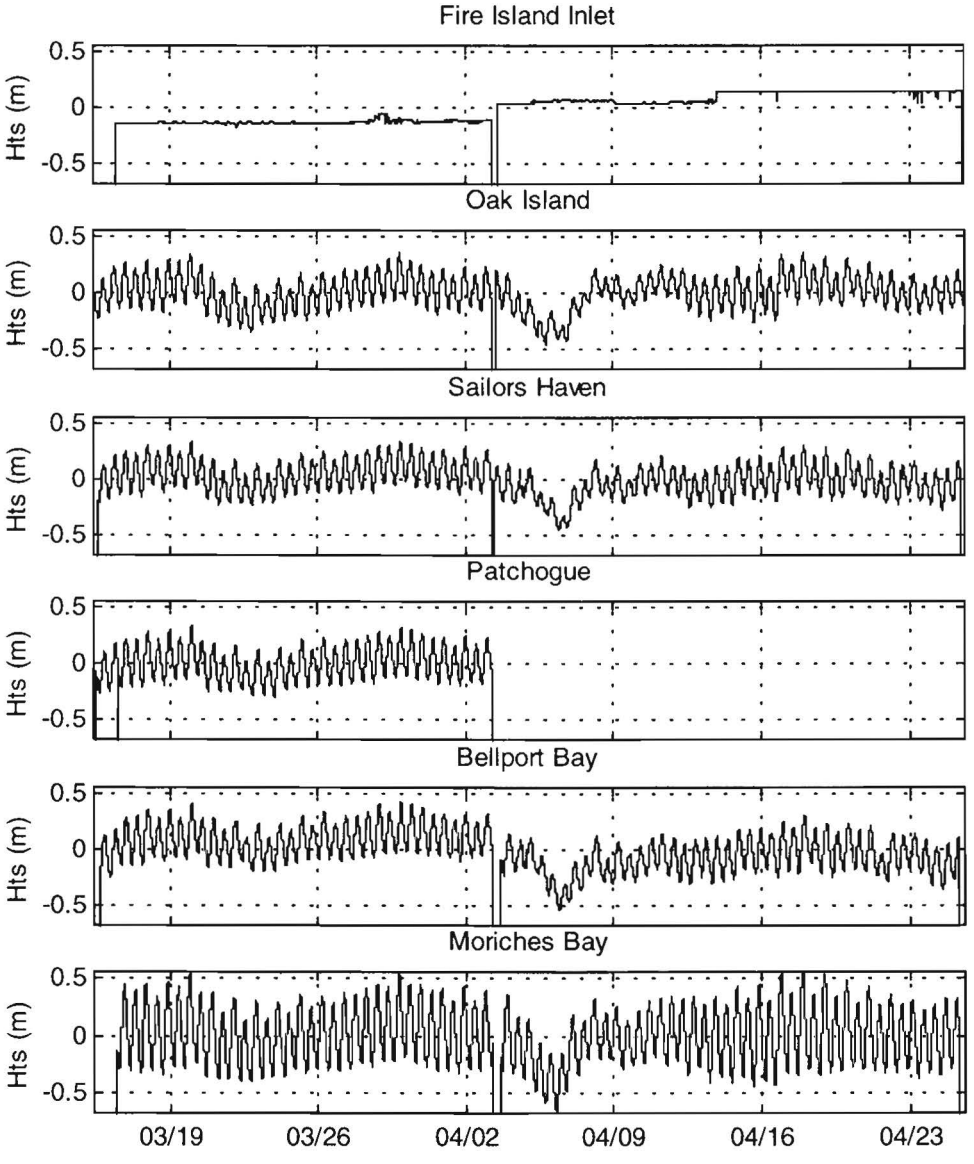

Figure 3. Tide measurements collected in field measurement program during March and April 1995. Values are in m relative to local mean sea level as calculated over the length of the deployment. The dropouts around 03 April represent instrument turnaround. Water depths in Fire Island Inlet were over sensor maximum depth. The Patchogue sensor was not replaced on second deployment. Note extra-tidal bay setdown centered around 06 April.

Initial model testing was composed of a calibration and a validation process. For calibration, the hydrodynamic model was run using observed external sea surface forcing and model free parameters were adjusted in order to optimize the comparison between model predicted and observed sea surface data in the interior of the bay. Validation was then performed by simulating a second time period using the previously determined parameters. In the absence of sufficient reliable salinity time series to calibrate salt transport simulations, earlier observations were used

to determine the inlet matching times and the horizontal mixing coefficient for salt, A_s, was set equal to A_H. In order to validate the model's ability to predict salinity changes, a simulation was performed with a breach in Westhampton Beach Island where the 1993 Little Pike's Inlet existed. The results of that simulation were then compared with the 1993 Little Pike's Inlet effects observations [Conley, 1999].

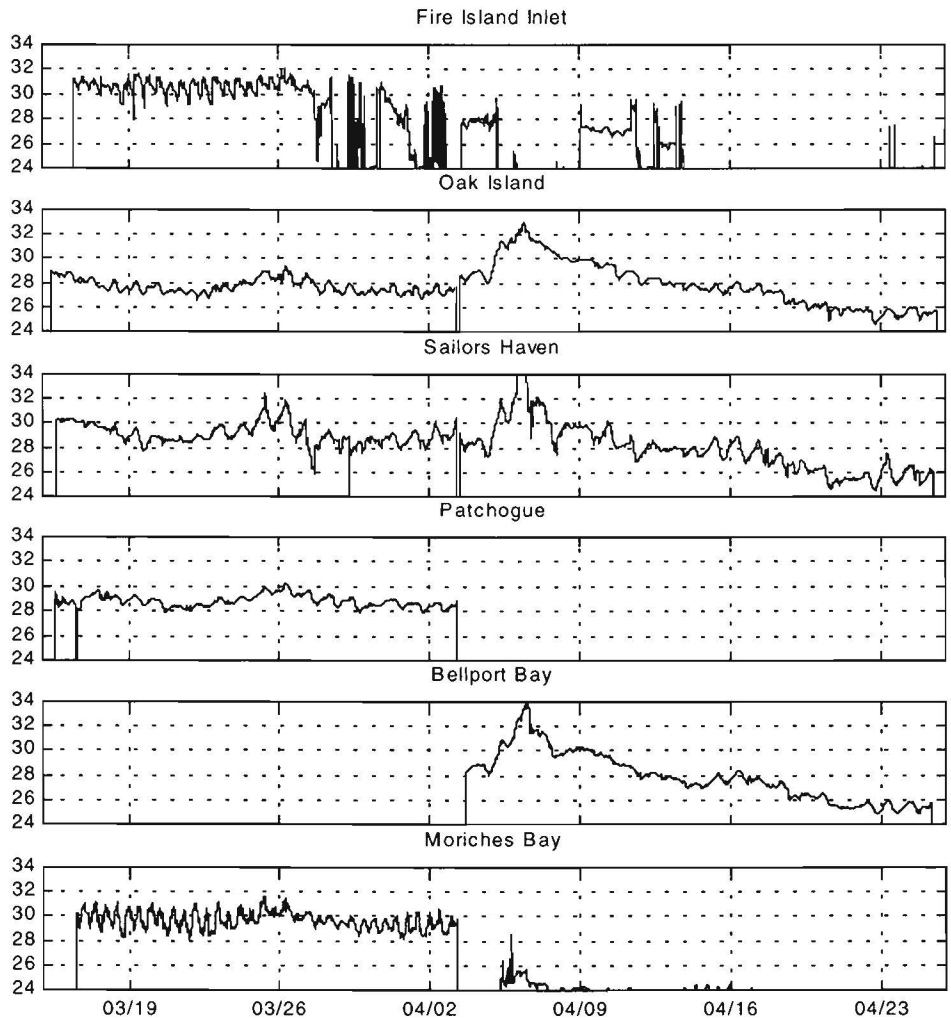

Figure 4. Salinity measurements collected in field measurement program during March and April 1995. Dropouts around 03 April represent instrument turnaround. Fire Island Inlet sensor was damaged midway through first deployment. Moriches Bay conductivity sensor was faulty on second deployment although the temperature sensor was operational. Extra-tidal salinity increase centered on 06 April can be seen to occur throughout the bay.

During the course of the Little Pike's Inlet study [Conley, 1999] a transfer function was developed which would approximate the tides at Westhampton Beach based upon the NOS data buoy tide measurements at Montauk Point. This function was used in the calibration and validation phases to estimate the ocean forcing signal at the inlet mouths because the measurement of sea surface elevation at Fire Island Inlet failed and no measurements were attempted at Moriches Inlet. This transfer function was of the form...

$$\eta(t) = \sum_{j=1}^{n} \beta_j A_j \sin(\sigma_j t + \phi_j + \theta_j) + \beta_r \eta_r(t) \qquad (1$$

where σ_j is the frequency of the jth tidal constituent, A_j and ϕ_j are the amplitude and phase at Montauk Pt. for these constituents and β_j and σ_j are the relative amplitude and phase for the transfer function. η_r and β_r represent the residual tide and the transfer function relative amplitude where residual tide is the sea surface fluctuations remaining after the harmonic tide has been removed. The standard deviation between the tide predicted using this transfer function and the observed tide is 6 cm. At Westhampton beach where the observed tidal range was found to be 1.1 m, the range calculated from the predicted tide and from the observed tide are within 3%. The ranges predicted from applying the procedure to Sandy Hook data and Montauk Pt. data agree within 1%. The tidal constituents used and the transfer function coefficients are shown in Table 1.

Table 1

Table of tidal constituents and transfer function coefficients used in computing inlet forcing tides for calibration and validation runs (A). Transfer function residual tidal coefficient relative to Montauk Pt. is 1.37.

Constituent	Tidal Speed (°/Hr)	Amplitude(m)	Phase (°)
M2	28.9841	1.888	63.1
S2	30	1.798	44.3
N2	28.4397	1.573	60.2
K1	15.0411	1.252	20
M4	57.9682	0.343	-62.4
O1	13.943	0.441	64.7
M6	86.9523	1.31	-58.1
MK3	44.0252	0.568	-20.9
S4	60	0.917	80.1
MN4	57.4238	0.248	-51.7
S6	90	1.109	-121.3
Mu2	27.9682	1.669	23.6
OO1	16.1391	1.564	-112
Lamd	29.4556	11.66	169.1
M1	14.4967	1.602	36.2
J1	15.5854	0.931	3.8
Rho1	13.4715	1.677	18.5
Q1	13.3987	1.795	19.8
2Q1	12.8543	0.889	51.1
2SM2	31.0159	2.969	2.6
M3	43.4762	8.638	58.6
2MK3	42.9271	0.526	-3.6
M8	115.9364	0.44	-123.9
MS4	58.9841	2.219	-89.5
Mm	0.5444	0.616	69

It is clear from Figure 3 that there are significant "tidal" fluctuations that are not part of the astronomical tide. Most of these fluctuations have a duration that is longer than the dominant

semi-diurnal tides. Such fluctuations are commonly referred to as "sub-tidal" however some of these non-tidal fluctuations may actually have a duration shorter than the semi-diurnal tidal period and so in this work, we shall refer to all such fluctuations a "extra-tidal". As no information existed regarding the relative mean sea level between the two inlets, and extra-tidal effects were not part of this project, a section of the tidal record that exhibited little sub-tidal variation was selected for testing. The longest such piece of data for which there was the greatest coverage at all measurement stations was a period of 9 semi-diurnal tidal cycles starting at 15:19 on 29 March 1995.

Table 2

Table of model-data comparisons for the calibration and validation runs of the model. The model was run with full ocean tide as forcing. Model free parameters were adjusted to optimize model data comparison during calibration run after which no adjustment occurred for validation run. Notice improvement in prediction for M2 tidal transmission even as rms elevation errors are slightly greater in validation run.

	Oak Island	Sailors Haven	Patchogue	Bellport Bay	Moriches Bay
Calibration Run					
RMS Elevation error (m)	0.059	0.039	0.044	0.047	0.055
Observed M2 amp (m)	0.147	0.131	0.142	0.137	0.246
Predicted M2 amp (m)	0.114	0.131	0.144	0.152	0.250
M2 Transm. Pred. Error (%)	-8.0	-0.1	0.5	3.8	1.0
Observed O1 amp (m)	0.030	0.036	0.035	0.037	0.034
Predicted O1 amp (m)	0.028	0.029	0.029	0.029	0.037
O1 Transm. Pred. Error (%)	-4.0	-16.6	-14.0	-16.6	4.8
Observed S2 amp (m)	0.030	0.035	0.044	0.049	0.093
Predicted S2 amp (m)	0.027	0.029	0.033	0.035	0.063
S2 Transm. Pred. Error (%)	-2.6	-5.1	-9.5	-11.8	-24.4
Validation Run					
RMS Elevation error (m)	0.081	0.063	0.059	0.065	0.07
Observed M2 amp (m)	0.155	0.151	0.163	0.170	0.304
Predicted M2 amp (m)	0.140	0.158	0.171	0.177	0.322
M2 Transm. Pred. Error (%)	-2.6	1.1	1.4	1.2	3.2
Observed O1 amp (m)	0.030	0.033	0.041	0.052	0.053
Predicted O1 amp (m)	0.034	0.040	0.046	0.050	0.086
O1 Transm. Pred. Error (%)	2.6	4.5	3.1	-1.1	20.6
Observed S2 amp (m)	0.033	0.032	0.032	0.041	0.035
Predicted S2 amp (m)	0.022	0.022	0.023	0.023	0.029
S2 Transm. Pred. Error (%)	-34.3	-30.7	-29.1	-58.8	-18.4

The model was originally forced at both inlets with the same simulated tidal signal for this period but it became apparent that a phase lag must exist between the two inlets. Trial and error indicated that introducing a lag of 0.8 hours between the forcing at Moriches Inlet and the forcing at Fire Island inlet gave the best match between model results and observations. This value compares favorably with the NOAA result that tidal lows at Fire Island Inlet lag the lows at Moriches Inlet by 40 minutes. The results of the final test are shown in Figure 5 where the

model predictions are plotted in solid lines and the observations are dashed. The elevation predictions take approximately 4 cycles to stabilize with the largest adjustments occurring during the first cycle. For this reason the first tidal cycle has not been presented in this figure.

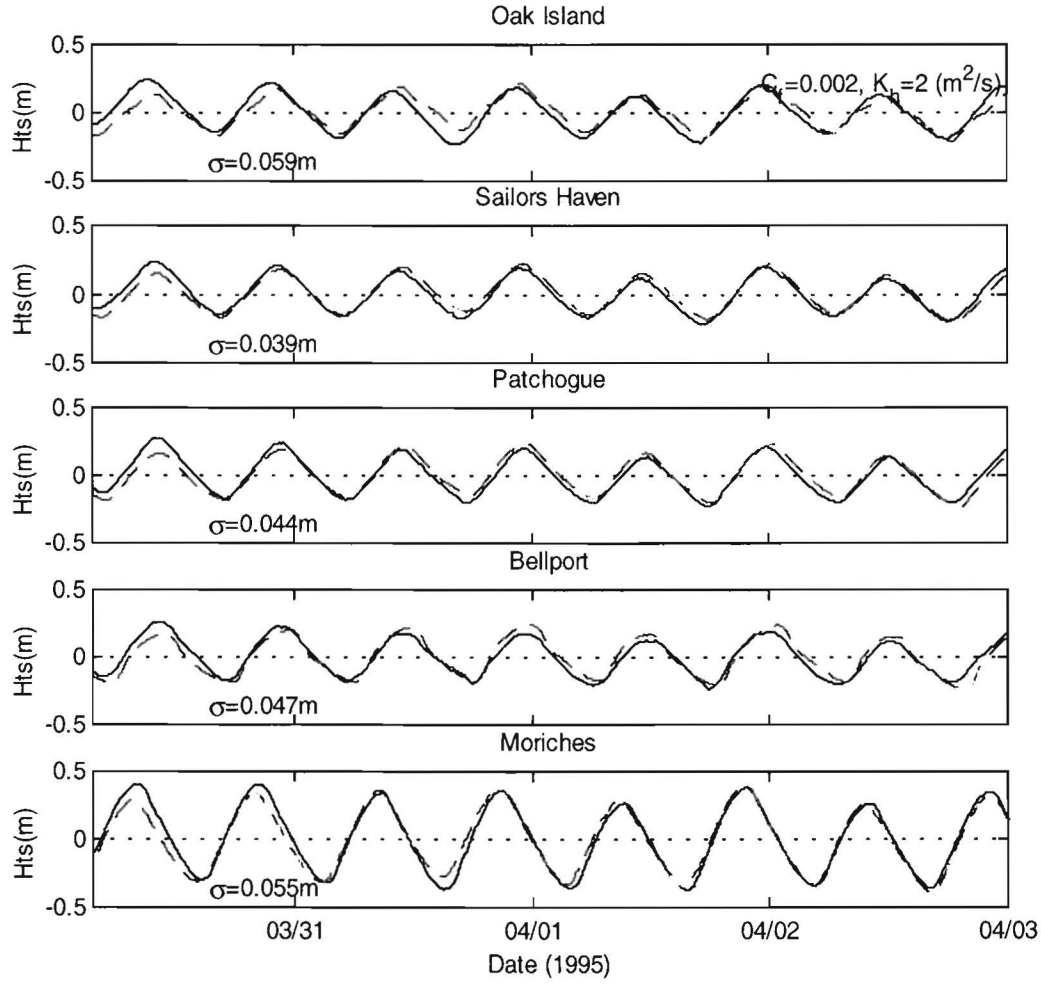

Figure 5. Comparison of model sea surface predictions (dashed lines) vs. field observations (solid lines). Data shown start one tidal cycle into simulation, which roughly corresponds 5, am on March 30. Data mean has been removed from all time series.

The time step for this run was 4s, which was the largest time step possible while maintaining model stability. Iterative calibration runs indicated that a typical bottom friction coefficient, C_f=0.002 and horizontal eddy mixing coefficient, A_H=2 m^2/s, produced the most favorable model-data elevation comparison although the results were not overly sensitive to these values. These parameters were used in all subsequent model runs. As can be seen in Figure 5, the comparison between model and observation is quite good, particularly for the period following the 50 hr. stabilization period. It is particularly revealing to observe the results at Oak Island. We can see that the simulations for tidal elevation are quite good at this location even with the nearby imposed solid boundary at South Oyster Bay. Table 2 confirms the good match between model simulations and observations with a mean standard deviation between model predictions and observations of 5 cm. The predictions of M2 tidal transmission are even better, typically accurate to within 2-3%. Once the model operating parameters had been determined, the independent validation run was performed using a similar length period of monitoring data.

This section, spanning the period 09:22 16 March 1995 – 13:36 21 March 1995, was less free of extra-tidal influence but of reasonable quality for comparison. The model-data comparison is shown in Figure 6 and selected parameters of model-data comparison are again presented in Table 2. While total elevation rms difference is worse for the validation run, the predictions of M2 tidal transmission are as good or better. This seeming dichotomy is due to the greater presence of extra-tidal events in the validation data. Following the calibration and validation procedure, all subsequent model simulations utilized a monochromatic semi-diurnal forcing (M2) with the regional mean tide range of 1.1m.

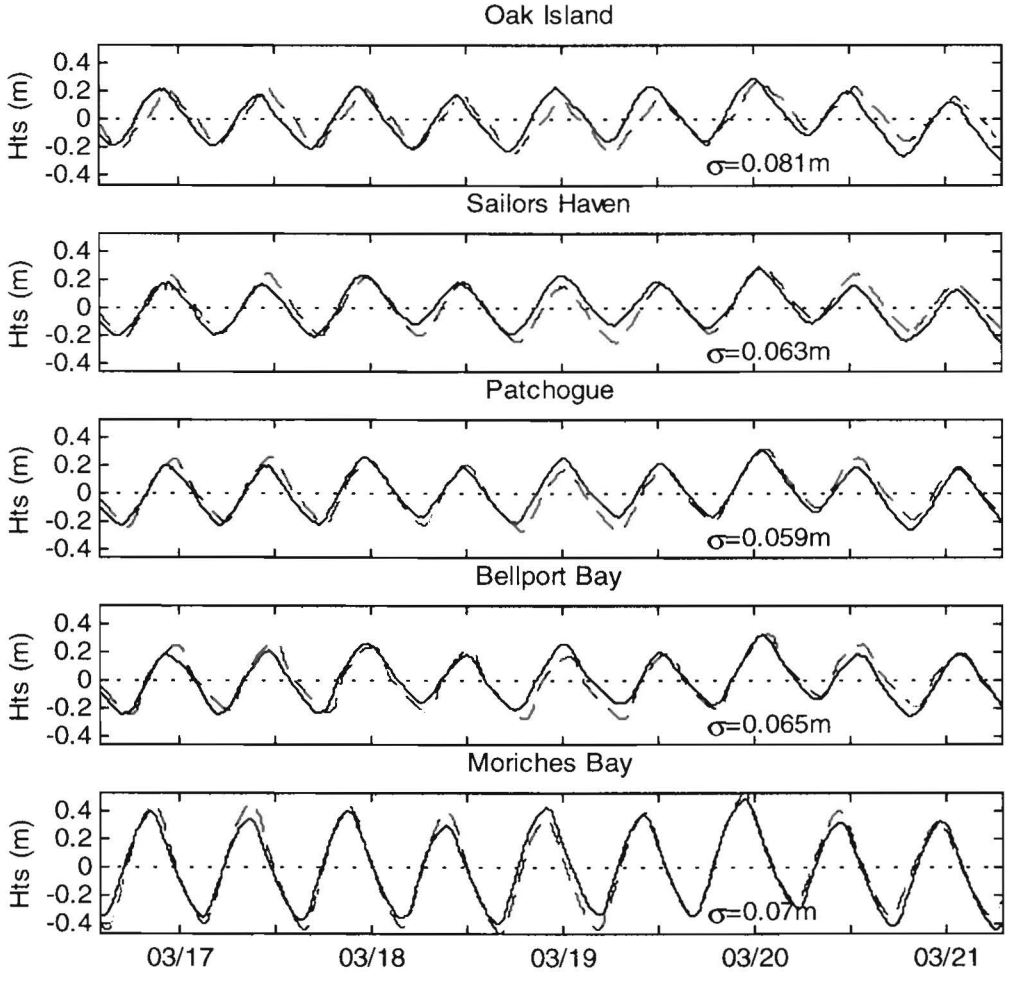

Figure 6 Comparison of model sea surface predictions (dashed lines) vs. field observations (solid lines) for validation run. Data shown start one tidal cycle into simulation and the data mean has been removed from all time series for the period plotted.

The second test involved introducing a breach at the location in Westhampton Beach Island where Little Pike's Inlet existed from Dec 1992 through Oct. 1993. Detailed bathymetric information regarding this inlet is not available so it is not possible to accurately reconstruct all the channels and flow obstructions that were present in the true breach. It was therefore decided to treat the breach as a simple gap in the barrier island and then adjust the dimensions of that gap so that the model tidal transmission prediction was approximately the same as that observed. This resulting gap so produced was the equivalent of a channel 150 m wide and 1.8 m deep. The

forcing point for this "gap" in the model was placed 2 grid points deep (300 m) in the model grid. No other alterations were made to the model bathymetry other than to increase bottom depths in Moriches Bay in front of the breach out to the point that the original bathymetry equaled or surpassed the 1.8m value. An analytical hydraulic model of Little Pike's Inlet [Conley, 1999] has shown that the inlet had the same resistance as an inlet 2 m deep, 260 m wide and 800 m long. Thus the gap employed in the model is seen to be of similar magnitude.

The Little Pike's Inlet tide measurements were collected at Speonk Pt. in Moriches Bay (Figure 1). These measurements showed that tidal transmission of the M2, semi-diurnal lunar tidal component, was 53% at this point without Little Pikes Inlet and 71% with the Inlet. Using the baseline (original geometry) monochromatic forcing results, the simulated tidal range is 59.3 cm. for the grid point corresponding to the Speonk Pt. measurement location. This result, which corresponds to a tidal transmission of 53%, represents an additional, independent, validation of the model. The corresponding values for the Pike's Inlet simulations are 86.0 cm or 78% transmission. The model breach geometry appears to be a little large in that the breach transmission rate is high relative to the observed rate. However, tidal transmission through inlets is a non-linear function of the tidal range. The observed results in Table 2 provide an example illustrating how higher tides experience significantly reduced transmission. The Pike's Inlet observed transmission rates are calculated on 28 day averages of full harmonic tides in which a significant portion of the tides have amplitudes higher than the 1.1 m range used in the simulations. While this may mean that the predictions and observation are even closer than they appear, the observed result suggests that the model over predicts the effects of such a breach.

With the simulated inlet characteristics fixed, the final model testing involved an independent validation of the model's ability to predict the relative changes in salt transmission. This was achieved by performing complete salt transport model simulations using the baseline model geometry and the Little Pike's Inlet geometry and comparing the results to the observed results. In the monitoring of the Little Pike's Inlet breach, it was observed that, following the closure of this breach, the salinity at Speonk Pt. dropped from a mean value of 30.3 ppt to a value of 29.0 ppt [Conley, 1999]. The model simulations predict a mean salinity at Speonk Pt of 29.5 ppt for the original geometry with salinity increasing to 31.0 ppt with Pike's Inlet. In the simulations, a predicted salinity change of 1.5 ppt compares very favorably with the observed change of 1.3 ppt. It is however worth noting that the absolute salinity levels in the model are at least 0.5 ppt higher than the observed. During this same period the salinity at the western part of Moriches Bay changed insignificantly, going from 28.5 ppt to 28.4 ppt. For this location the model predicts a change from 31.6 ppt to 31.5 ppt. These results validate that the model accurately predicts the magnitude of changes in salinity even when the absolute level of the salinity is simulated with considerably less precision. The models poorer ability to predict absolute salinity levels is discussed elsewhere and is likely due to two separate effects. The first of these has to do with the homogenization of the freshwater input so that no real point sources exist. Such an effect would be most strongly seen near stream mouths such as near the Forge River data collection point used in these comparisons. The second is the fact that the model does not account for long period extra-tidal effects which may be as important as tides, or more so, in affecting salinity levels in the bays.

Model Operation

Early tests of the models clearly indicated that model tidal elevations quickly came to equilibrium, showing little change after 3-4 tidal cycles. Salinity results on the other hand were never observed to come to a final equilibrium and took on the order of 3000 hr. simulated time to approach a steady state. For this reason, the simulations were split into two steps. In the first

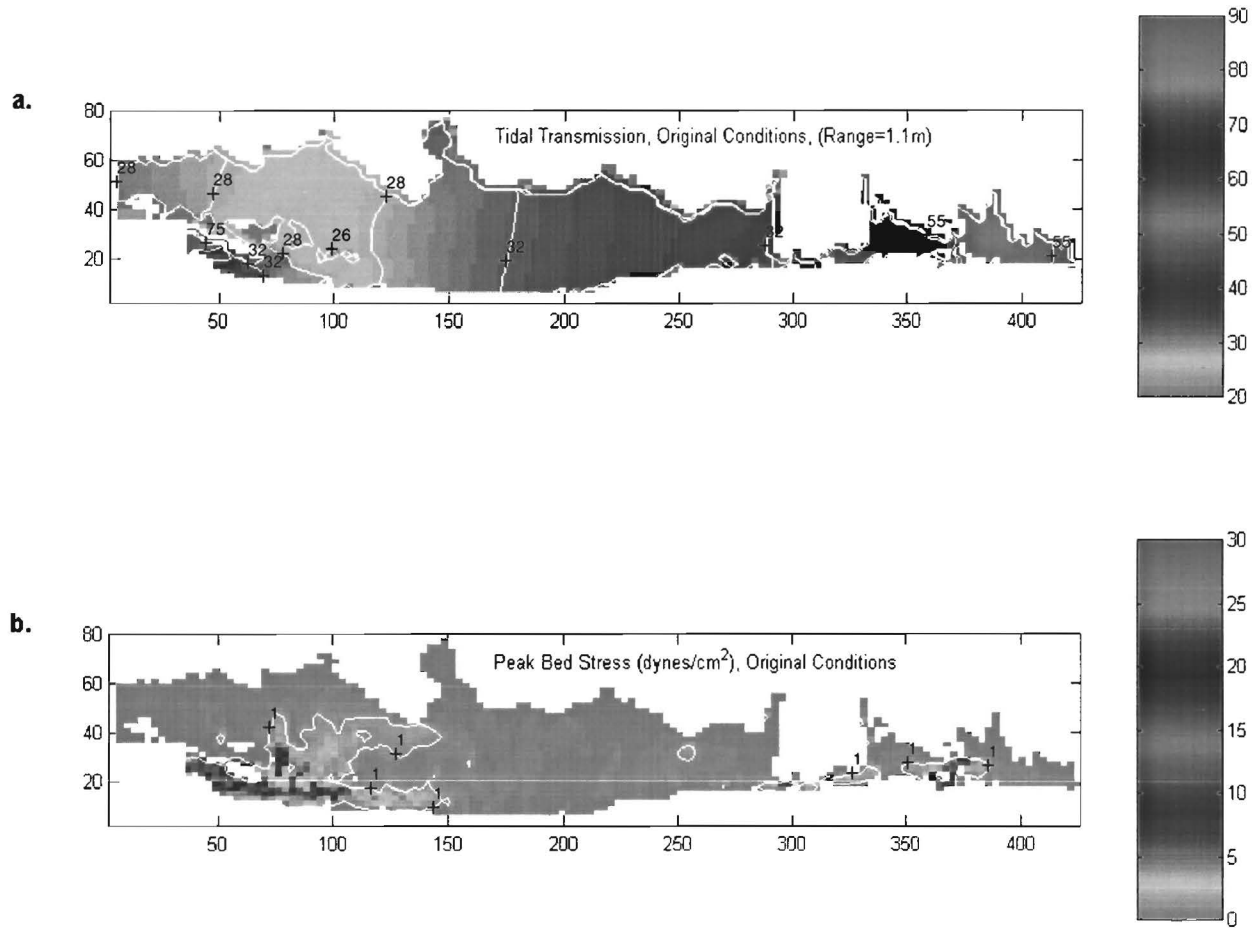

Figure 7. Plots indicate level of tidal transmission (% of ocean forcing tide observed at location) (a.) and peak bed stress (b.) results for the simulation with the original geometry. Color represents the level of the respective variable predicted at each location and the color bar to the right provides scale. Contours in a. highlight transmission patterns but are not indicative of extreme values. The contour in b. indicates the 1 dyne/cm^2 threshold for the mobilization of fine sand. Horizontal and vertical scales are in units of model grid points with 150 m. spacing between grid points.

step, the model was stripped of salt transport components (although freshwater inflow was still accounted for as a volumetric inflow). These simulations were run for 63 hours with intensive output archiving (dt=1/24th cycle) over the final full tidal cycle. The initial conditions for all the simulations were the results of a long (10's of cycles) preliminary simulation using the original bathymetry. These simulations were all forced by a sinusoid with a period of 12.42 hr. and an amplitude of 0.55 m (range = 1.1 m) which is representative of the mean tidal range on the south shore of Long Island.

The salt simulations were run similarly but for considerably longer periods. A base start file for all simulations was created by running the model with the original geometry and a uniform salinity distribution of 28 ppt for approximately 6000 hr. of simulated time. The model was stopped when the change in salinity at any single grid point was less than 0.005 ppt/tidal-cycle. The final output of this simulation was then used as the initial conditions for all simulations. All geometries were then run for a simulated time of 2981 hours or 240 tidal cycles. This run time was sufficient to ensure that the greatest salinity change in any cell was less than 0.01ppt/tidal cycle for all tests. The mean change was several orders of magnitude less than this with the majority of the changes occurring at the closed western extreme of Great South Bay.
In total, simulations for 4 different geometries were performed; the current, "original" geometry and 3 simulated breaches. The locations of the 3 simulated breaches were Pike's Beach on Westhampton Beach Island, and Old Inlet and Barret Beach on Fire Island. The first site was selected due to the actual development of Little Pike's Inlet at that location and the existence of monitoring data from the breach period, which could be used to validate the model. The Old Inlet location was chosen due to the historically recent existence of inlets at this location [Leatherman, 1989] and the present occurrence of cross-island overwash. Barret Beach is currently one of the narrowest points in the island and as such represents a relative weak spot. It is also representative of the narrow, west-central portions of Fire Island in which the bay side of the island is no longer part of the Fire Island Inlet entrance channel, the bay side bathymetry is relatively deep and the tidal phase lag with the ocean is at a maximum. Thus the simulations at Barret Breach are representative of a breach anywhere from Sailor's Haven to Davis Park.

RESULTS

Tides

Figure 7a is a color plot of the tidal transmission in Great South and Moriches Bays as predicted by model simulation based on the original geometry. In such plots, the color indicates the level of the variable of interest. The value of the color can be determined by examining the legend to the right of the plot. A limited number of contours have been added to the plot to provide a direct level reference but the contours present should not be taken as an indication of the minimum or maximum levels. In this case, tidal transmission is defined as the percentage of the forced tidal signal that is transmitted into the bay. This quantity was calculated by taking the sea surface elevation predictions at individual grid-points, interpolating these predictions to 60 s time step and then using the difference between the minimum and maximum elevations to represent the local tidal range which was then normalized by the forcing range (1.1m). It should be recalled that the formal definition for the mean range [Pugh, 1987] is the distance between mean low water and mean high water. For model output, forced with steady conditions, these two definitions are equivalent but field data must always be treated according to the latter definition.
Figure 7a provides a general picture of tidal transmission in Great South Bay. The highlights of which are; a rapid reduction in the tidal range through the long and sinuous channels of Fire

Island Inlet such that the transmission has dropped to 30% at the exit of the inlet, relatively constant tidal range (~0.35 cm) over all of Great South Bay with a mean transmission near the above cited 30%, a general east to west gradient of decreasing tidal transmission of approximately 4% with the minimum near the inlet discharge and slightly higher tides at the western end, and a large range gradient between Great South Bay and Moriches Bay with tidal ranges in the western end of Moriches Bay of order 60% confronting Great South Bay tides of 30%. Qualitatively, these results appear to agree with earlier simulations as well as with the field measurements outlined in Table 3. The simulations do seem to somewhat under-predict the increase of the tides towards Oyster Bay (Oak Island) and this may have to do with the boundary condition at this end of the model.

Table 3

Comparison of observed and predicted tidal transmission. Transmission represents local tide range as a % of ocean tidal range, which is 1.1 m for the simulations but varies for the measurements. Field data are derived from observations in Figure 3 and are only representative of original geometry. Locations are shown as stars in Figure 1.

	Field Data	*Original Simulation*	*Pike's Inlet Simulation*	*Old Inlet Simulation*	*Barret Beach Simulation*
Oak Island	34%	31%	31%	36%	37%
Sailors Haven	32%	34%	34%	39%	38%
Patchogue	36%	37%	37%	40%	39%
Bellport Bay	36%	39%	39%	36%	41%
Moriches Bay	63%	66%	83%	67%	66%

The tidal current pattern associated with this tidal transmission is shown in (Figure 8). The circulation pattern is relatively straight forward with currents and elevations at the inlets relatively in phase (slack currents appear to occur at phase of 0 and π which correspond to occurrence of mid-tide level at the inlet). Flood tides enter both inlets and then diverge to fill the surrounding basins. Great South Bay has three current channels, one in which the current effectively reverses direction and hugs the northern shore of Jones Beach Island filling the basin adjoining South Oyster Bay, one which swings north through the various flood tidal shoals and islands before heading east again as Great Cove is approached and the third path which represents the direct continuation eastward of the inlet channel. Moriches Inlet appears to have 2 major current patterns, one that flows due north from the inlet and then spreads east and west along the northern edge of the bay and the second pattern that flows westward only along the southern edge of the bay. Ebb tide is ostensibly simply the reverse of this pattern. It is worth noting that Moriches Bay feeds Great South Bay on the flood tide and drains it on the ebb. The spatial distribution of the residual transport associated with these currents is shown in Figure 9. The averaging process used to develop these figures results in confused mean transport in the inlets. The high velocities in the inlets have mean transports which change direction within the dimensions used to average the velocities so that the mean transport vectors do not appear coherent. The residual circulation in the interior of the bay is quite clear however. Major features include permanent cyclonic eddies (anti-clockwise flowing) in eastern Moriches Bay, Bellport Bay, Patchogue Bay and northern and southern Nicoll Bay. Anti-cyclonic eddies (clockwise flowing) occur in western Moriches Bay as well as in the basin below Great Cove and in mid-Nicoll Bay. A net transport is seen from Moriches Bay into Great South Bay. Net transports also exist out of both inlets with the sum of the transport equaling the freshwater input into the bays.

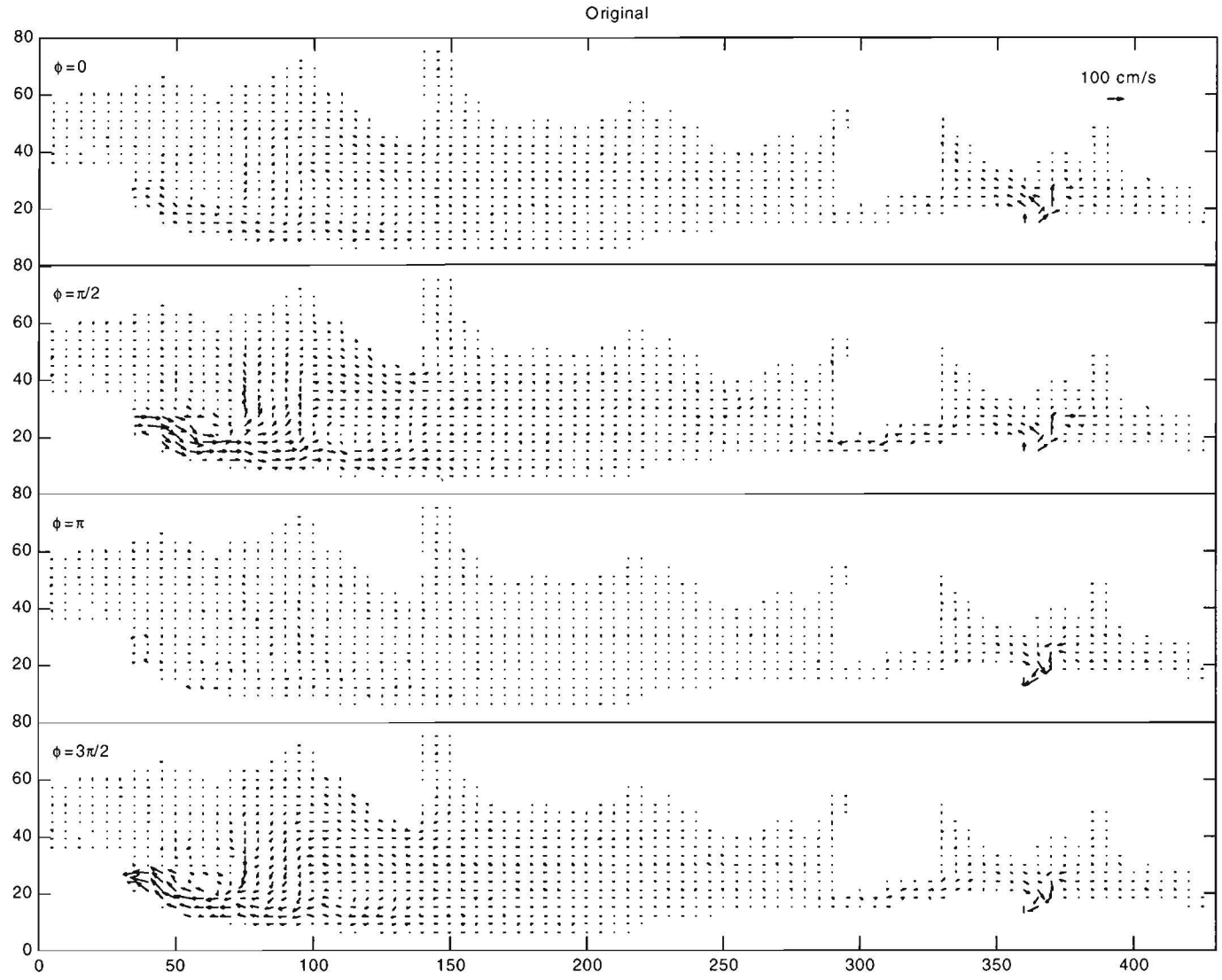

Figure 8. Tidal current velocities for original simulation at four different phases (ϕ). A phase of ϕ=0 corresponds to mid-tide (z=msl) on a flooding tide at Fire Island Inlet. Vectors indicate magnitude and direction of velocity and represent the spatial average over three grid points across bay and 5 points along bay.

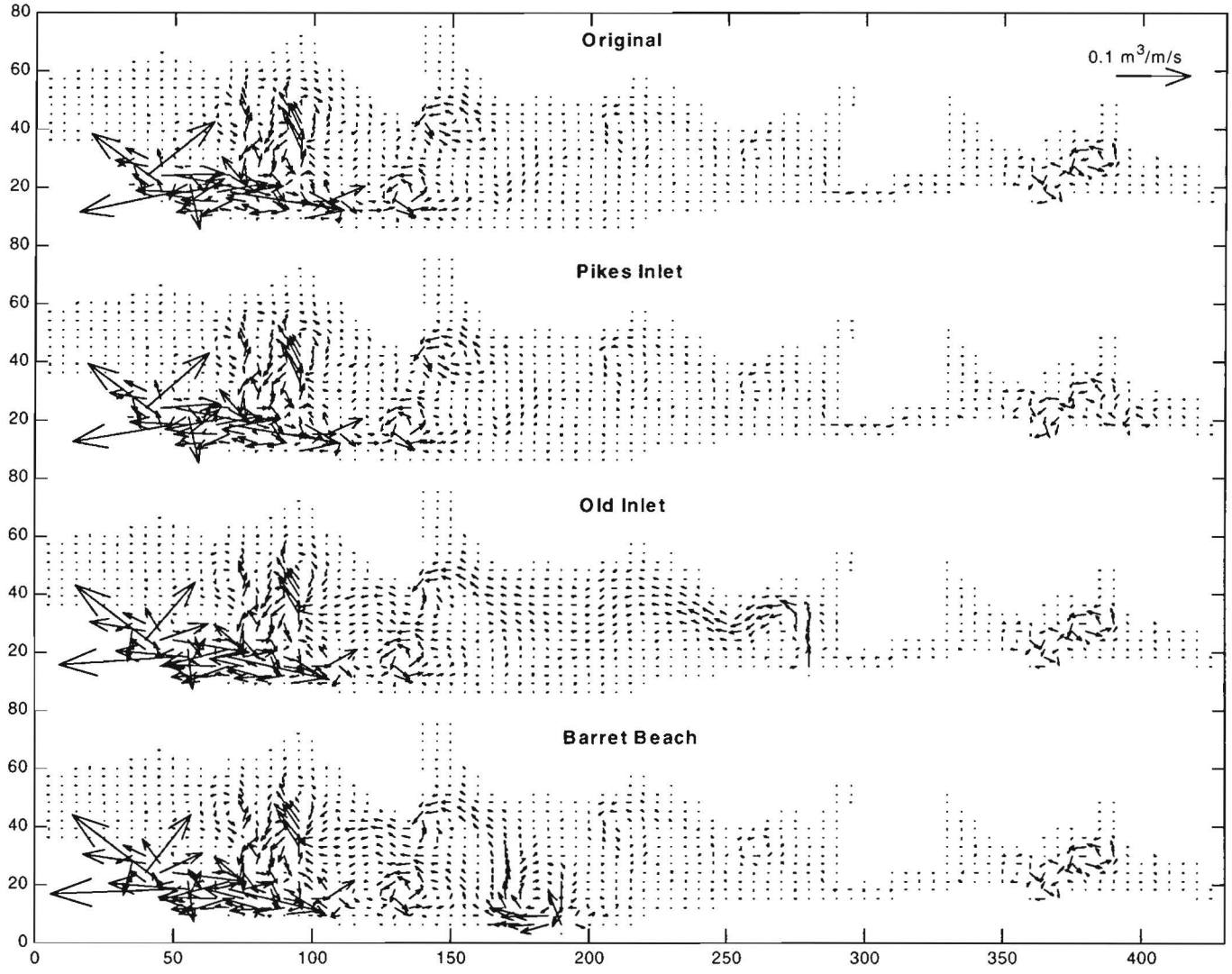

Figure 9. Net transport for all four simulations. Vectors indicate magnitude and direction of transport. Values are calculated over one tidal cycle and are spatially averaged over three grid points across bay and 5 points along bay. Confusion near Fire Island Inlet is due to significant net transport gradients over spatial scales smaller than the averaging scales.

Figure 7.b represents a plot of the magnitude of the maximum bed stress experienced throughout a tidal cycle. Here bed stress, $\vec{\tau}_b$, is calculated from a quadratic stress relation

$$\vec{\tau}_b = C_f |\vec{u}| \vec{u} \qquad (2$$

where $\vec{u}$ is the velocity vector and C_f, the friction coefficient, was 0.002 as in the model simulations. As would be expected from (2), the bed stress pattern closely shadows the tidal current pattern, with regions of high bed stress mirroring regions of strong currents. The 1 dyne/cm^2 contour has been plotted on Figure 7b. This value is representative of the critical threshold for the mobilization of fine sand grains. Theoretically, all areas inside this contour should experience tidal currents that are strong enough to move fine sands and silts at least once during a tidal cycle. While the threshold for erosion of clays is influenced by factors in addition to grain size, it is reasonable to assume that freshly deposited muds would also be mobilized in these regions. Thus the bottom composition in these regions is probably coarser material. While many other factors may affect bottom composition outside this contour, the probability that it is mud or a mud-sand mixture is much higher. As the figure indicates, the higher stress regions are confined to the inlet channels, the Smith Point narrows and a large section of Great South Bay south of Great Cove where the tidal currents exiting Fire Island Inlet diverge.

The results of the tidal transmission tests for the simulation with a breach at Little Pike's Inlet (hereafter referred to as the Pike's Inlet simulations) are shown in Figure 10. The general pattern of tidal transmission (Figure 10a) is little changed from that discussed for the original geometry. The only difference immediately discernible is apparent higher transmission in all of Moriches Bay with the greatest transmission occurring in the eastern half of Moriches Bay. This pattern is easier to see in Figure 10b, which is a plot of the differences in tidal transmission between the Pike's Inlet simulation and the original. This figure clearly shows that this breach has almost no effect on tidal transmission into Great South Bay. Tidal transmission is however increased significantly in Moriches Bay, beginning with a 5% increase in the narrows and increasing steadily eastward. The highest increases of over 25% occurred throughout the eastern half of the bay. These results, as have already been discussed, are consistent with observations.

Among the concerns surrounding the effects of a breach on the environment in the back bays is the impact on benthic communities. In order to begin to estimate what such impact might be, the changes in bottom stress have been plotted in the final panel of this figure (Figure 10c). In this figure, changes in the temporal mean bed stress magnitude ($\langle |\vec{\tau}_b| \rangle$) have been calculated at each grid point and normalized (divided) by the spatial mean value for the original simulation. Thus, this plot represents changes in mean gross stress experienced by the bed, which we shall designate as bed scour to denote the lack of directional information in this quantity. For the Pike's Inlet simulation, we can see that practically all changes occurred in Moriches Bay with a pattern that varied greatly depending on location. In much of the channeled region of Moriches Bay and the Smith Point Narrows, there was a greater than 30% increase in scour due to the increased tidal flow to that area. This increase rose to over 60% as Moriches Inlet was approached at which point there was a reversal in which scour decreased due to the reduce tidal flow into eastern Moriches Bay from Moriches Inlet. That flow was replaced by the new flow through the simulated breach that of course exhibits greatly enhanced bed scour around the breach. Small isolated regions of increased bed scour are seen in Great South Bay and these appear to arise from a small adjustment to a resonant tidal structure in Great South Bay that is slightly modified by the new conditions. A similar type of adjustment is observed in all the simulations and does not appear to represent major changes in the flow structure. Peak stress results indicate no changes in peak stress in Great South Bay. As would be expected from Figure 10c, peak stress magnitudes within Moriches Bay (Figure 11a) have been altered but changes in

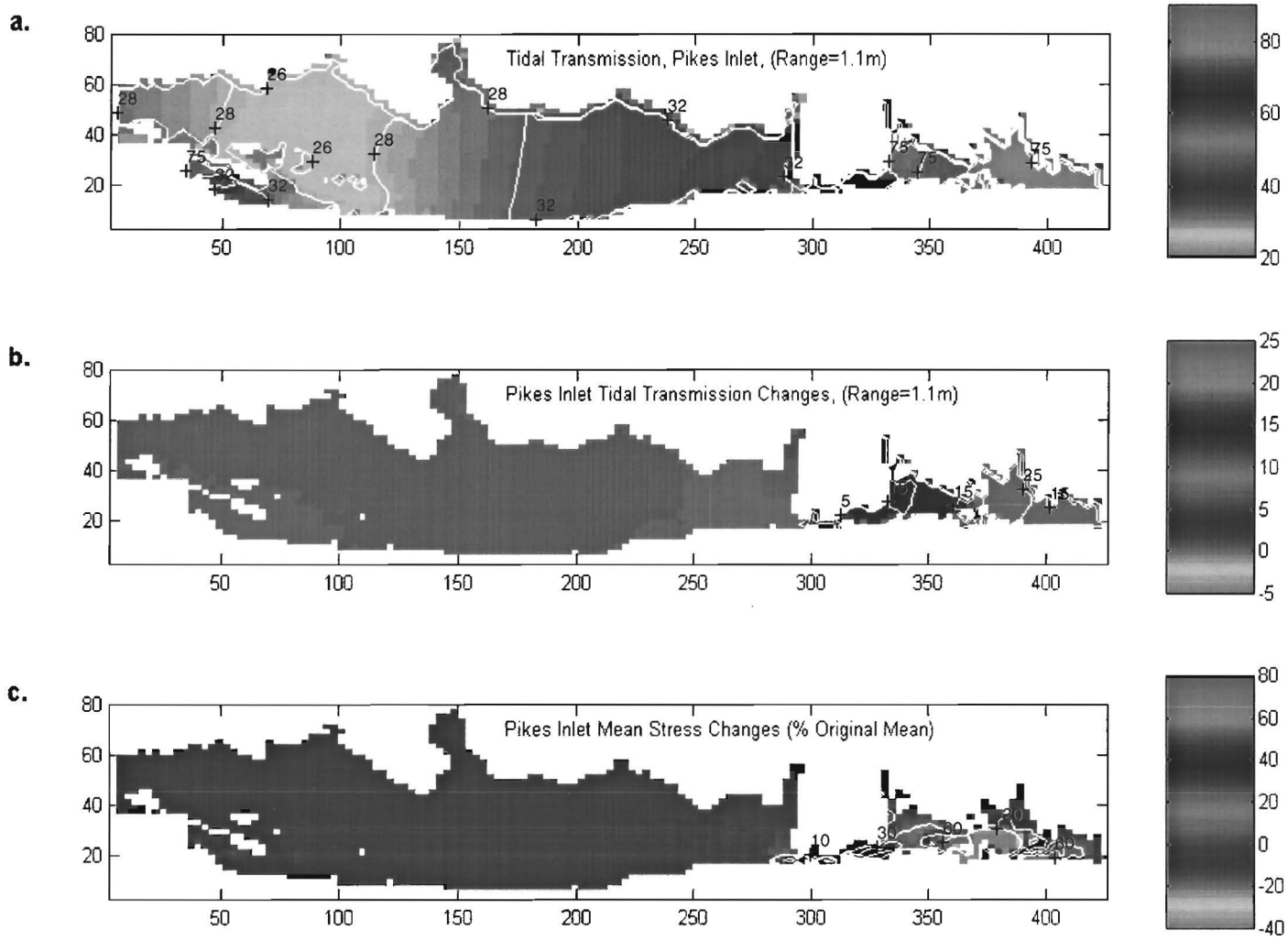

Figure 10. Results of tidal simulation for Pike's Inlet and comparison with results for original geometry. Color represents level of tidal transmission (% of ocean forcing tide observed at location) (**a**.), changes in transmission relative to original geometry (**b**.) and changes in local mean gross stress (expressed as a percentage of the original total mean gross stress) (**c**.). Color scale for **a**. is the same as in Figure 7**a**. Contours are not indicative of extreme values. Horizontal and vertical scales are in units of model grid points with 150 m. spacing between grid points

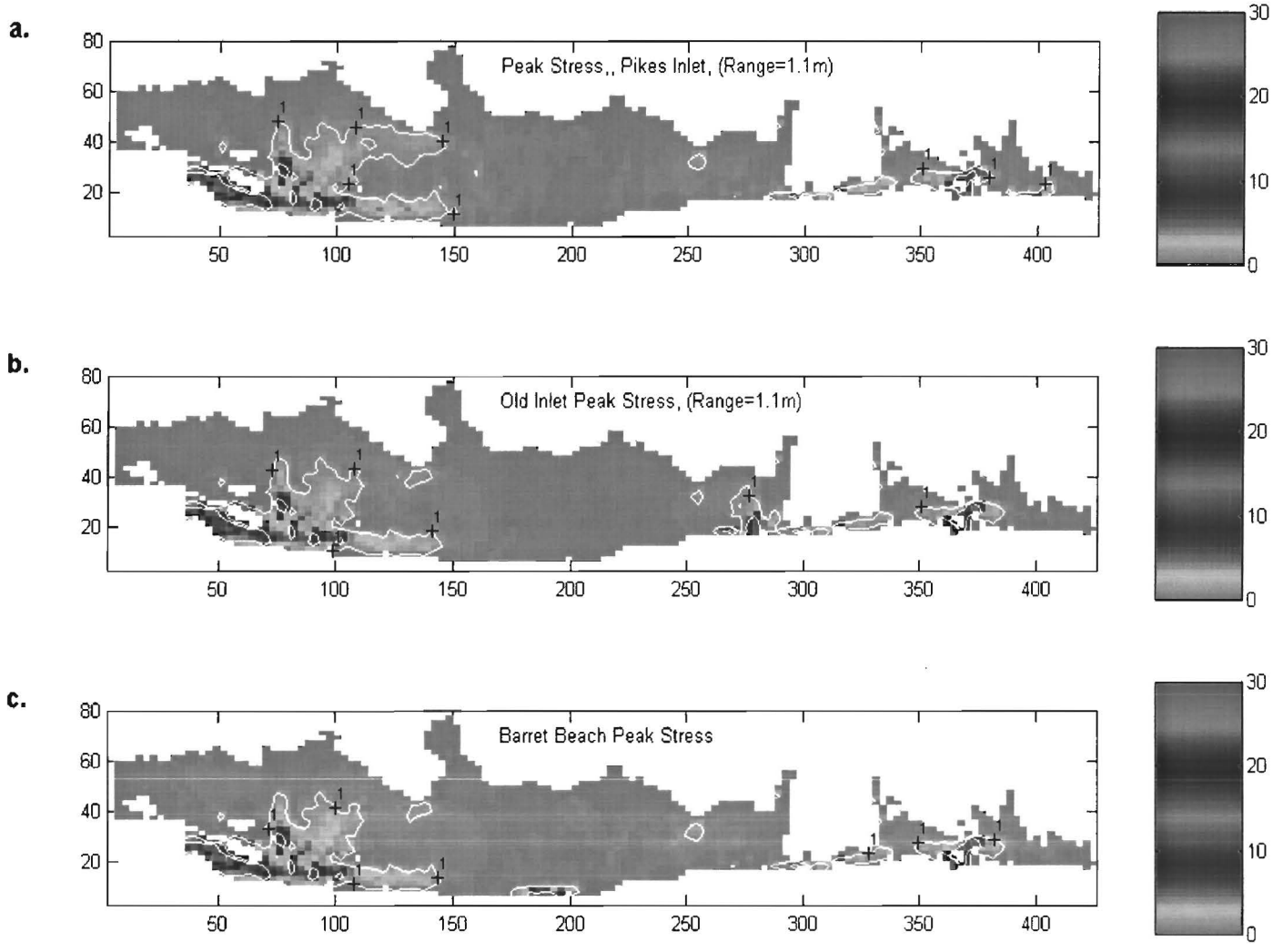

Figure 11. Peak bed stress results for (**a.**) Pike's Inlet, (**b.**) Old Inlet and (**c.**) Barret Beach simulations. Values are calculated using (1) where $C_f = 0.02$. The contours indicate the 1 dyne/cm^2 threshold for the mobilization of fine sand. Compare the results with those from the original geometry in Figure 7**b**. Horizontal and vertical scales are in units of model grid points with 150 m. spacing between grid points.

the coverage of the 1 dyne/cm^2 contour (Figure 7b) are small. A 1 km retreat of the contour can be seen at the edge east of Moriches Inlet as well as the development of a new exceedance zone around Little Pike's Inlet which closely mirrors the 30% change contour in that zone.

The tidal circulation plots (Figure 12) exhibit the enhanced flow to the west of Moriches Inlet as well as the severely diminished flow to the east. The tidal currents into and out of Great South Bay also appear to be slightly stronger although the net transport (Figure 9) appears unchanged. The only apparent change in the net transport pattern is the transformation of the eastern Moriches eddy into a mean circulation from Little Pike's Inlet to Moriches Inlet.

We have now seen the effects of a breach in the barrier islands in Moriches Bay, namely increased tides throughout Moriches Bay and complicated patterns of bed scour throughout the bay with generally increased gross bed stress but some locations of decreased stress. However, almost all of these effects are confined to Moriches Bay with little impact predicted for Great South Bay. It is time therefore to take a look at what effects might be predicted for a breach in Fire Island with a direct opening into Great South Bay. The first such simulation that will be considered is for the case of a breach at Old Inlet.

The pattern of tidal transmission seen in Figure 13a is a rather different picture than the original presented in Figure 7. The east-west gradient appears to have disappeared with relatively even transmission of 35% occurring across the basin except for near the inlet discharges for both Fire Island Inlet and the Old Inlet breach where transmission drops down to around 32%. The pattern in Moriches Bay appears not to have altered. The details of the changes with respect to the original conditions are shown in Figure 13b. Here we see that a majority of Great South Bay experienced transmission increases of 4%. Seemingly paradoxically, the shallow area immediately surrounding Old Inlet experienced a reduction in transmission on the order of 4%. This local reduction results from the transformation of this zone from a dynamically inactive (Figure 8) potential energy reservoir to a dynamically active (Figure 14) source of kinetic energy. No significant change is observed in the tidal situation for Moriches Bay.

The bottom scour changes associated with a breach at Old Inlet (Figure 13c) reflect the new basin filling pattern for this simulation (Figure 14). In particular, it would appear that the filling and draining of Great South Bay by flow through Fire Island Inlet is greatly reduced. Flow through the new breach, as well as the reduced tidal flow through the Smith Point narrows, appears to make up for this reduction (Figure 14). This is reflected in Figure 13c where we see a large increase in the mean bed stress in the region surrounding the new inlet. This increase is as much as 80% and crosses the width of the bay with values of 20% or greater. The results from maximum bed stress calculations (Figure 11b) indicate that a new region exceeding the 1 dyne/cm^2 threshold has developed around the new breach and extends across much of the width of the bay at this point. This increase is accompanied by a related reduction in scour through the center section of the bay. This decrease is greater than 10% through a section approximately half the size of the bay and attains values as high as 60% in some locations. A large reduction in the 1 dyne/cm^2 threshold region also occurs in this area. The eastern boundary for this region has retreated to approximately grid point 115 except for the southern channel where it has retreated to grid point 140 (Figure 11b). A reduction in bed stress through the Smith Point Narrows reflects the reduction in exchange between Moriches and Great South Bay. Net transport (Figure 9) undergoes a major alteration with the presence of this breach. The stationary eddies in Bellport, Patchogue, and Nicoll Bays, have all been replaced by a relatively large mean current from Old Inlet to Fire Island Inlet. Net transport in Moriches Bay and western Great South Bay are largely unaffected although the mean transport from Moriches Bay is substantially diminished.

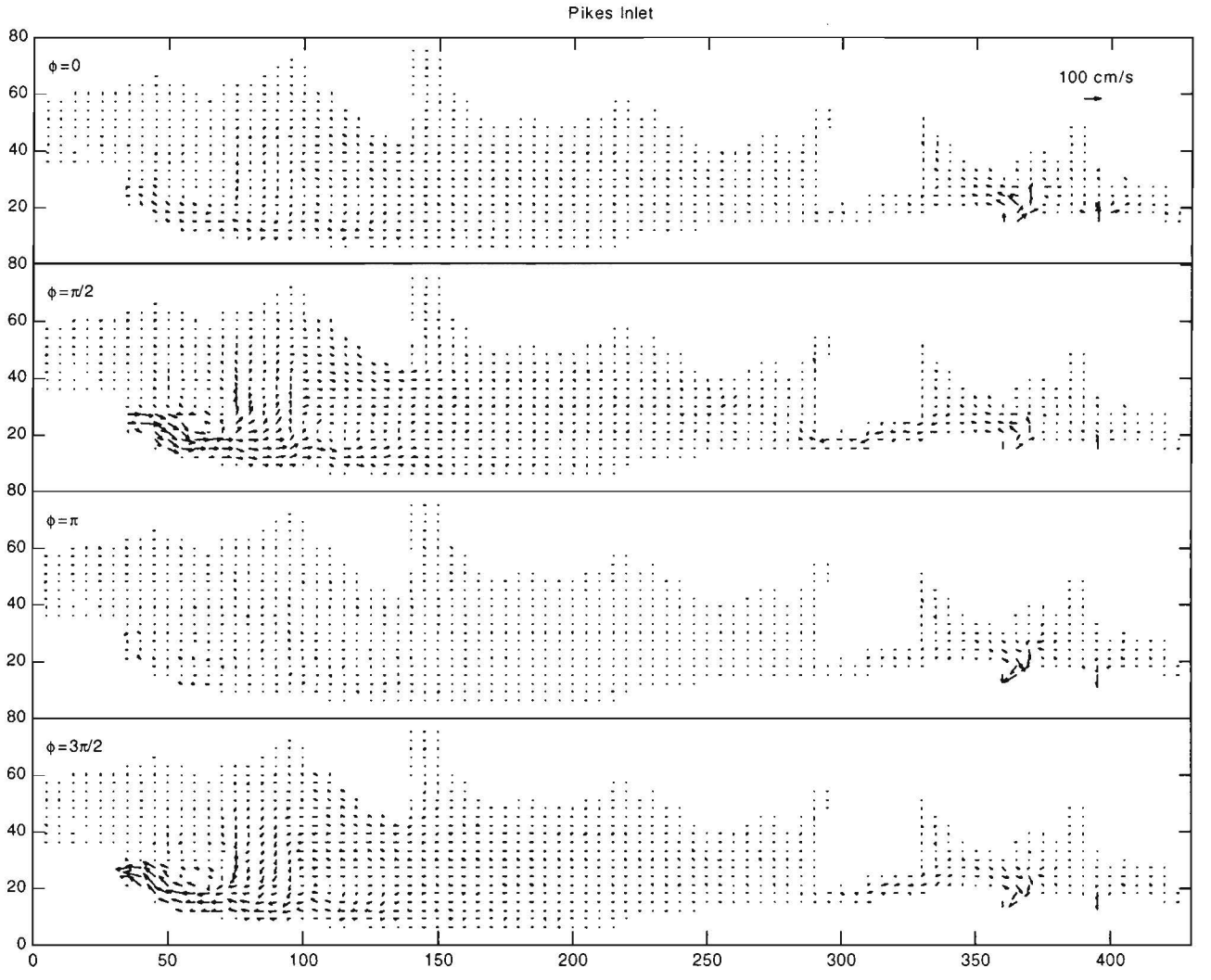

Figure 12. Tidal current velocities for Pike's Inlet simulation at four different phases (ϕ). A phase of ϕ=0 corresponds to mid-tide (z=msl) on a flooding tide at Fire Island Inlet. Vectors indicate magnitude and direction of velocity and represent the spatial average over three grid points across bay and 5 points along bay.

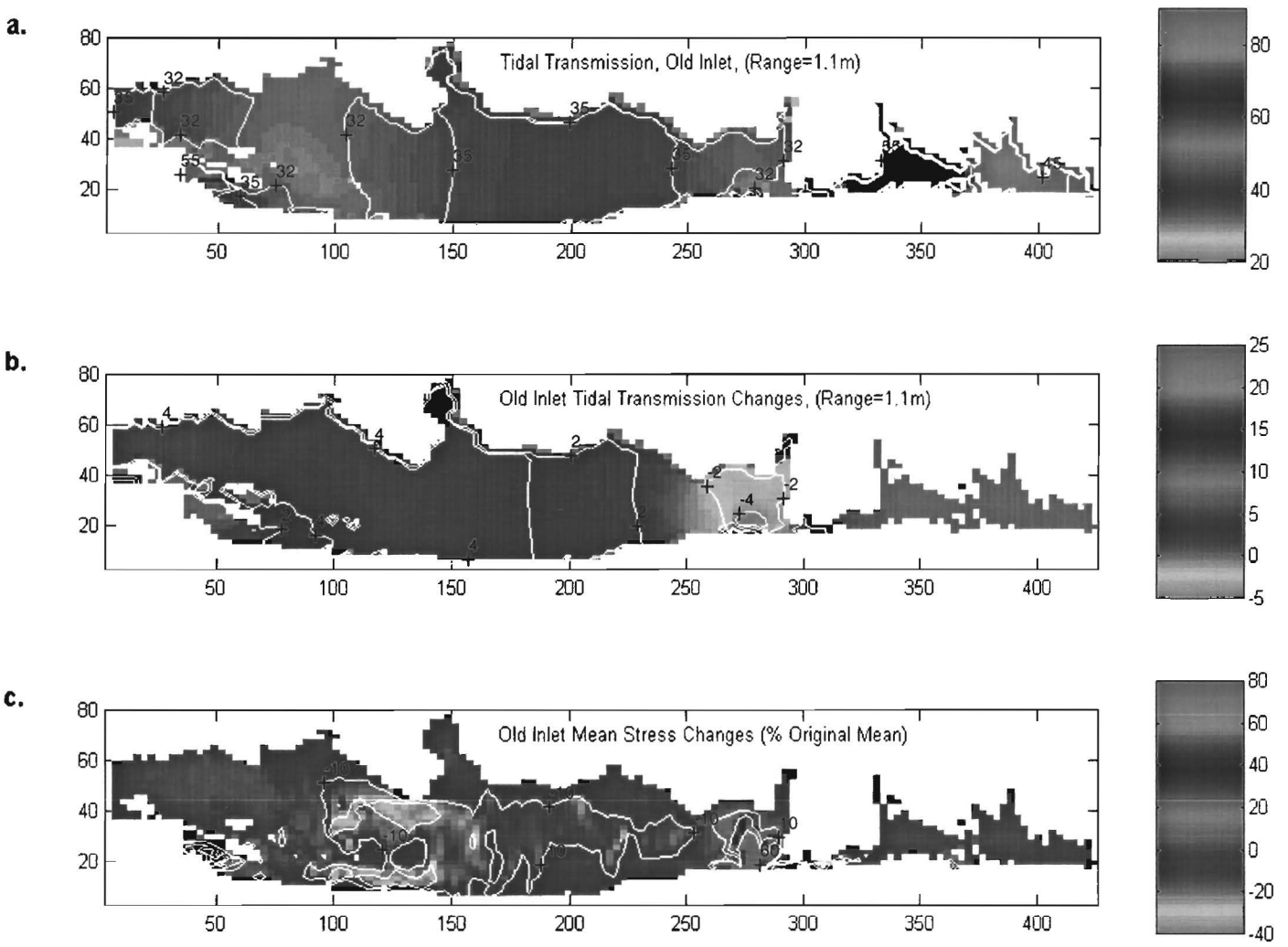

Figure 13. Results of tidal simulation for Old Inlet and comparison with results for original geometry. Color represents level of tidal transmission (% of ocean forcing tide observed at location) (**a.**), changes in transmission relative to original geometry (**b.**) and changes in local mean gross stress (expressed as a percentage of the original total mean gross stress) (**c.**). Color scales are all the same as in Figure 10. Contours are not indicative of extreme values. Horizontal and vertical scales are in units of model grid points with 150 m. spacing between grid points

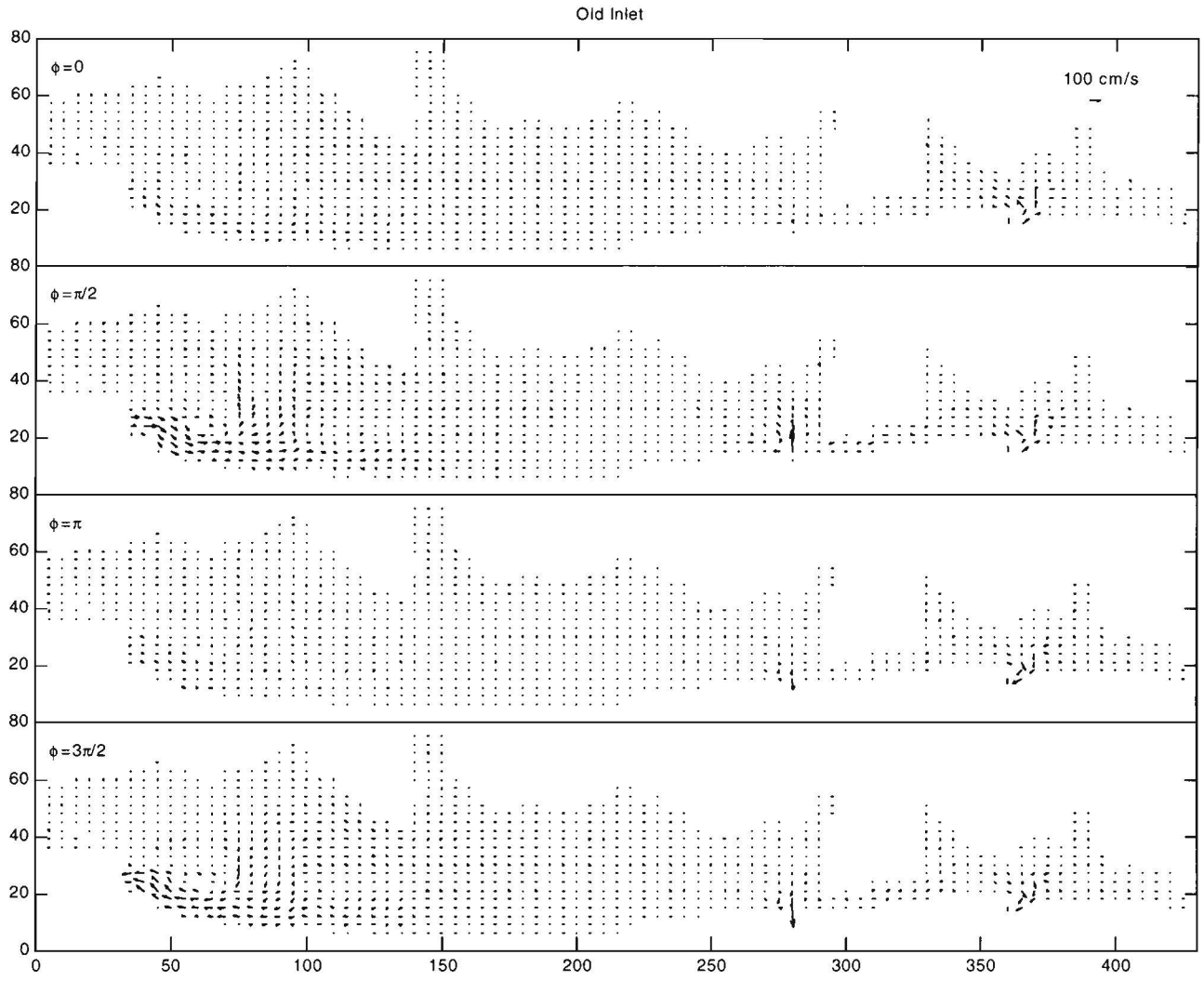

Figure 14. Tidal current velocities for Old Inlet simulation at four different phases (ϕ). A phase of ϕ=0 corresponds to mid-tide (z=msl) on a flooding tide at Fire Island Inlet. Vectors indicate magnitude and direction of velocity and represent the spatial average over three grid points across bay and 5 points along bay.

The final simulated breach occurs at Barret Beach, approximately halfway between Democrat Point and Smith Point. Similarly to the Old Inlet breach, this breach provides an alternative method to fill the eastern section of Great South Bay although the entrance is much further westward. As a result, the bay tidal ranges mirror the original pattern of an east-west gradient of decreasing tidal range with a slight increase in the western extremes (Figure 15a). This is reflected in Figure 15b where a relatively uniform increase in tidal regime is observed throughout the bay. The scour pattern is very similar to that for the Old Inlet breach although the extent of the alterations is greatly reduced. Once again mid-bay decreases in bed stress are observed reflecting the separate sources for the east and west basins as well as increased scour surrounding the new breach at Barret Beach. The reduction in the mid-bay bed stress threshold limit region (Figure 11c) is identical to that described for Old Inlet and the only additional region exceeding the threshold is the limited area surrounding the new inlet (Figure 11c). Tidal current patterns for this simulation (Figure 16) are relatively similar to the original geometry (Figure 8) with the addition of a mid-bay source which somewhat diminishes the original flow into Nicoll Bay but increases the flow into Bellport Bay. The tidal exchange with Moriches Bay is substantially diminished and the mean transport from Moriches Bay is practically erased (Figure 9). A reasonably large net transport is introduced from Barret Beach looping up through Nicoll Bay and down out into Fire Island Inlet.

Salinity

For all the salinity results presented here, the convention will be to exhibit the distribution present at the time of slack tide after ebb at Fire Island Inlet. Figure 17a shows this salinity distribution for the baseline simulation with the original geometry. This distribution appears reasonably predictable given the tidal circulation presented earlier. Higher salinity water is seen to occur near the inlets with a freshening away from them as would be expected considering the source of salt. The distribution also tends to indicate the circulation patterns with fingers of high salinity following the three current pathways issuing from Fire Island Inlet.

Pockets of fresh water in the simulation highlight two regions of the bay where little circulation occurs and lateral mixing is not sufficient to spread salinity. The first of these occurs along the northern shore of Nicoll Bay where salinity appears to drop below 25 ppt and suggests a region of low recirculation. The other section is along the western boundary adjoining Oyster Bay. The circulation patterns for both of these areas (Figure 8) show very small tidal velocities and the net transport (Figure 9) indicates practically no recirculation. While the latter region may be partly due to model boundary conditions, the former appears to be a true zone of relative stagnation. The simulation also suggests that the net transport from Moriches Bay into Great South Bay (Figure 9) is a source of salt which leads to a high salinity pocket in eastern Great South Bay.

The salinity data collected during the field measurement section of this experiment is of relatively low precision (2-3 ppt) and represents a rather short period of time considering the amount of time required for the bay to arrive at equilibrium. The Suffolk County Department of Health has been periodically collecting salinity data in Great South Bay since 1977. Figure 18 is a map showing the mean salinity values at many of the stations that are sampled. Table 4 lists this data along with the mean value for the field measurement sites and the corresponding values for the four simulations. There is considerable discrepancy between the field data and the simulation estimates. These differences can be broken into three types. The first difference has to do with a relative underestimate of the salinity through out the central basin of Great South Bay. This behavior is exemplified by the differences associated with stations C through D as well as at Sailors Haven. Most probably this underprediction is derived from two sources. The first would appear to be an over estimation of the matching time so that salinities of the entering

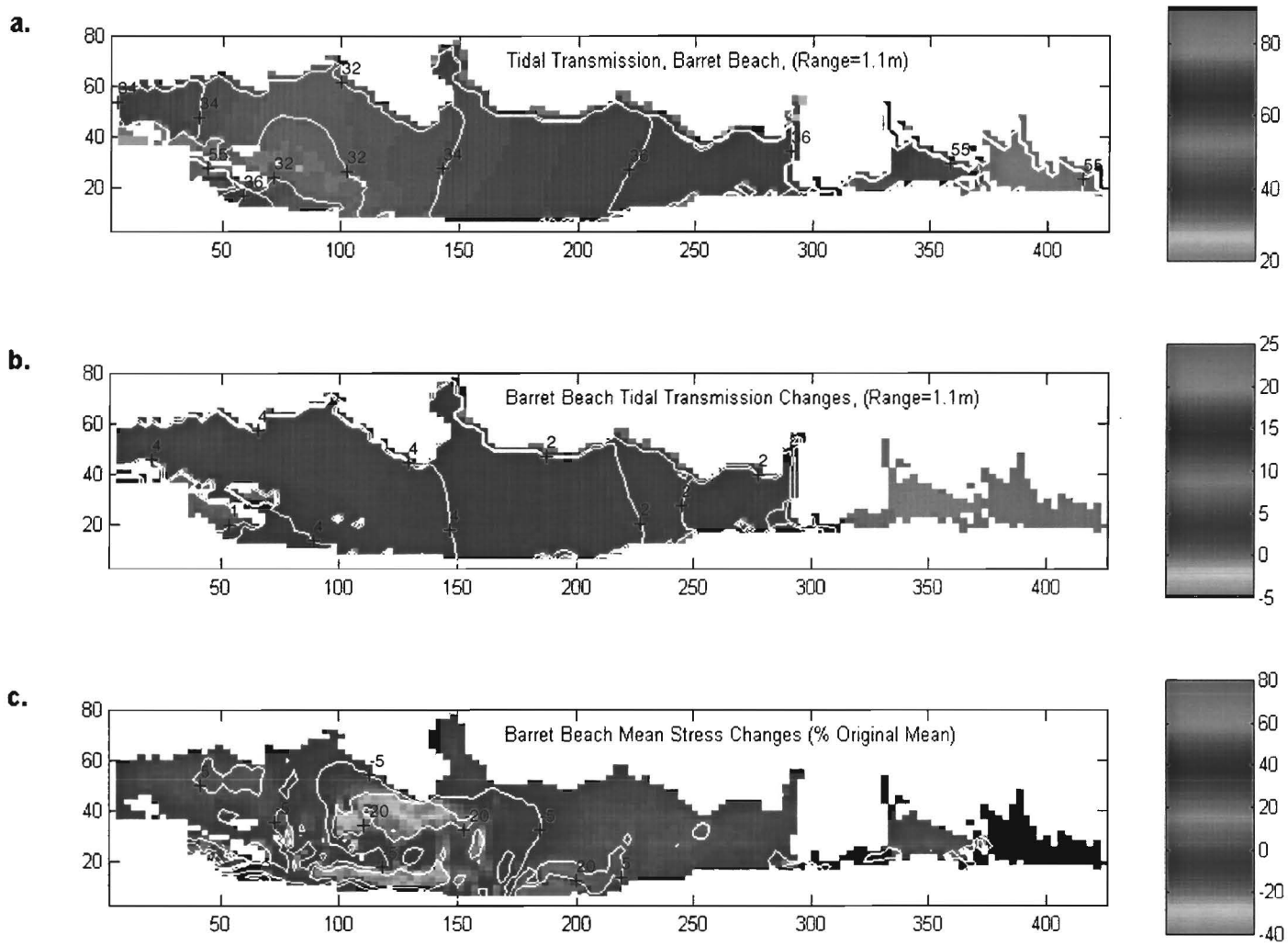

Figure 15. Results of tidal simulation for Barret Beach and comparison with results for original geometry. Color represents level of tidal transmission (% of ocean forcing tide observed at location) (**a.**), changes in transmission relative to original geometry (**b.**) and changes in local mean gross stress (expressed as a percentage of the original total mean gross stress) (**c.**). Color scales are all the same as in Figure 10. Contours are not indicative of extreme values. Horizontal and vertical scales are in units of model grid points with 150 m. spacing between grid points.

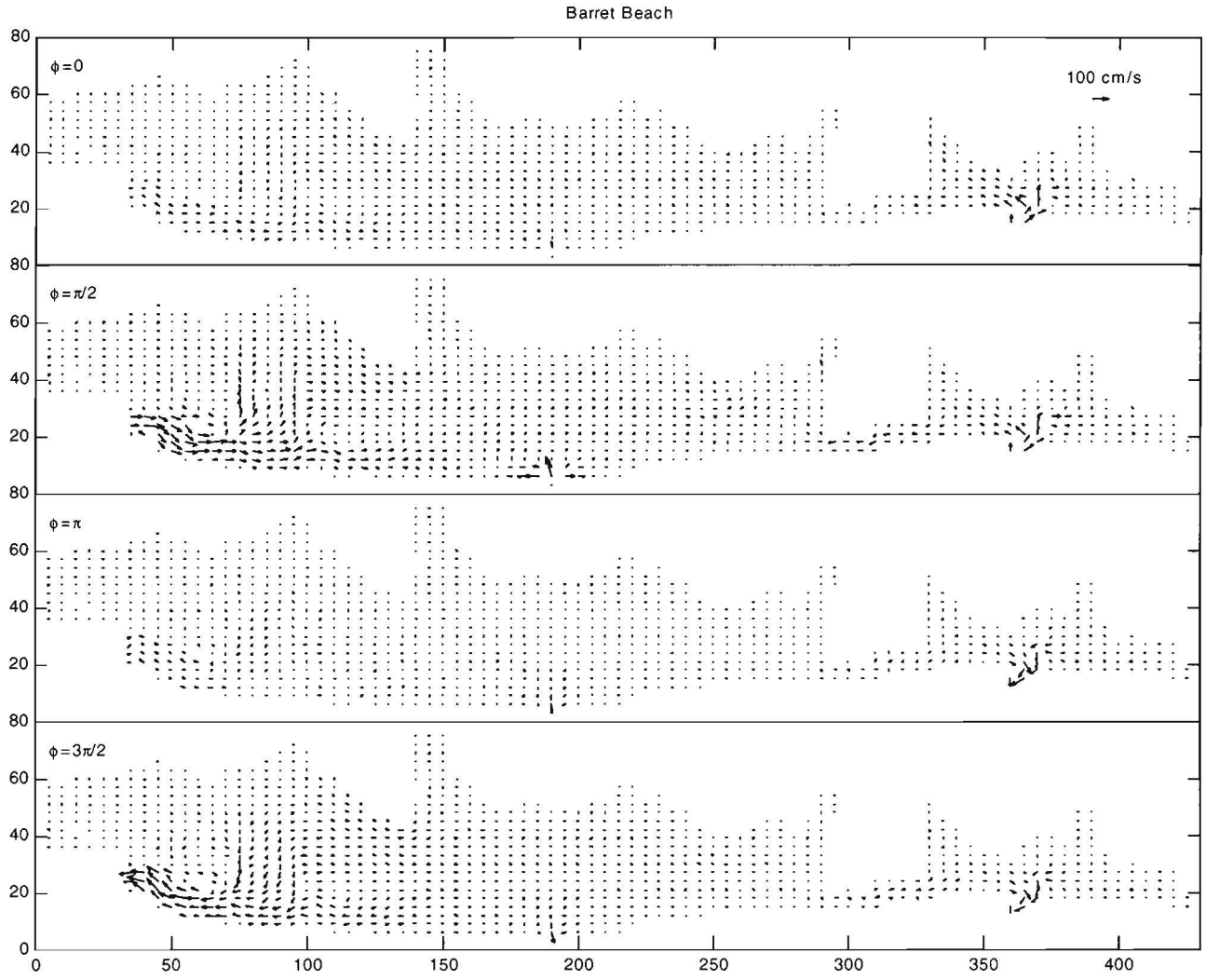

Figure 16. Tidal current velocities for Barret Beach simulation at four different phases (ϕ). A phase of ϕ=0 corresponds to mid-tide (z=msl) on a flooding tide at Fire Island Inlet. Vectors indicate magnitude and direction of velocity and represent the spatial average over three grid points across bay and 5 points along bay.

flood tide (salt source) are too low. This is supported by the underestimation of values at station D, which is directly influenced by this flow. Such an effect would be strongest near the inlet and tend to diminish with distance. The second effect has to do with the fact that other extra-tidal effects, which may be much more efficient at transporting salt into the bay, are not simulated in the model. This issue will be examined further under discussions but this effect might be most important for the regions furthest removed from strong tidal flows where tidal mixing is weak. Together these two effects could explain the differences between observed and estimated salinity values in this central basin.

Table 4

Comparisons of measured and simulated mean salinity values. The means for the first 5 locations are calculated over the first two weeks of deployment as shown if Figure 4. The values for stations A-O represent an approximately 20 year mean. The locations of these stations are indicated in Figure 18.

	*Field Data**	*Original Simulation*	*Pike's Inlet Simulation*	*Old Inlet Simulation*	*Barret Beach Simulation*
Oak Island	27.8	21.9	23.5	24.3	24.9
Sailors Haven	29.3	26.1	26.2	30.3	31.4
Patchogue	29.0	26.2	25.2	30.4	25.6
Bellport Bay	-	30.6	30.2	31.7	26.9
Moriches Bay	29.8	31.5	31.5	31.3	31.2
Station A	28.76	15.20	18.47	19.34	20.05
Station B	28.12	18.78	19.84	20.90	21.45
Station C	27.36	24.21	25.60	26.51	26.99
Station D	29.57	27.51	27.93	29.30	29.63
Station E	26.40	25.68	25.81	28.37	28.53
Station F	28.37	25.16	25.31	28.66	29.17
Station G	27.53	26.13	26.42	29.76	30.59
Station H	27.12	24.93	24.81	30.14	30.98
Station I	25.30	23.71	23.41	27.78	27.81
Station J	25.76	25.84	25.55	31.09	30.81
Station K	24.76	24.93	24.23	28.56	24.48
Station L	25.93	26.59	25.48	31.60	30.91
Station M	24.80	28.17	27.21	31.06	25.97
Station N	23.23	30.76	28.67	31.00	24.94
Station O	25.22	31.36	31.60	31.63	30.97

These explanations do not however account for the exceedingly low salinities estimated in the western boundary of Great South Bay (e.g. stations A, B and Oak Island). It is most likely that these are a result of the boundary condition here which fails to account for an attached body of high salinity and perhaps over predicts the stagnant nature of this bay. In a model of Great South Bay which included a forcing term in South Oyster Bay, Wong [1981] observed instantaneous tidal flux through the bay at Robert Moses Causeway (east-west grid pt. # 65) which was approximately 1/3rd the magnitude of that through Fire Island Inlet. In the present study that ratio was approximately 1/10th. Thus while the closing off of the western boundary may not have affected tidal elevation greatly (Figure 5) it is likely that salt exchange processes are poorly represented here. This clearly represents a weakness in the model but in the absence of more detailed information on the exchange processes at this boundary, it was not possible to treat this region differently. The final type of salinity discrepancy occurs in the eastern end of

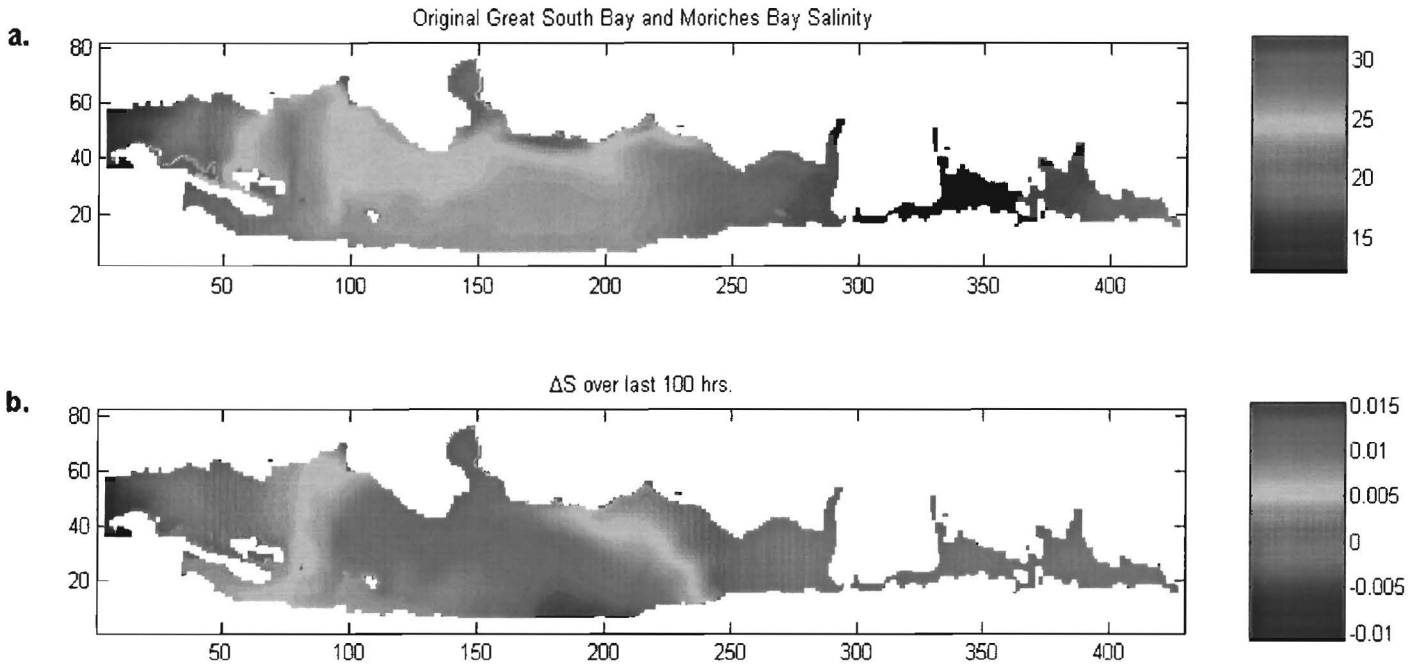

Figure 17. Salinity results for the simulation with the original geometry. Part **a**. shows the bay wide distribution of salinity occurring during slack tide after ebb at Fire Island Inlet and **b**. shows the changes in this value over the final 100 hr. of simulation. Color represents the local value in salinity units and the color bars to right provide the scale. Horizontal and vertical scales are in units of model grid points with 150 m. spacing between grid points.

Great South Bay where the estimates are far too saline (e.g. stations M, N and O). There are two possible sources for this error, one would be an over estimate of the transport and mixing from Moriches Bay. However, considering the tidal transmission validation results and the relative success of the Pike's inlet simulation; it is likely that this is a not a large problem. More likely, most of this high salinity arises from the failure of the model to appropriately account for the Carmans River, which enters Bellport Bay to the east. According to Pritchard and Gomez-Reyes [1986], the drainage of the Carmans River alone accounts for approximately 25% of the freshwater input into Great South Bay. Thus, while the rest of the north shore of Great South Bay has a relatively even distribution of small and medium size waterways which are probably well represented by a constant line source, the representation of freshwater input into Bellport Bay by such a technique underestimates the input by at least a factor of two. The spatial extent of this effect can be estimated by considering that the predictions for stations J, K and L appear to be reasonable values (Table 4).

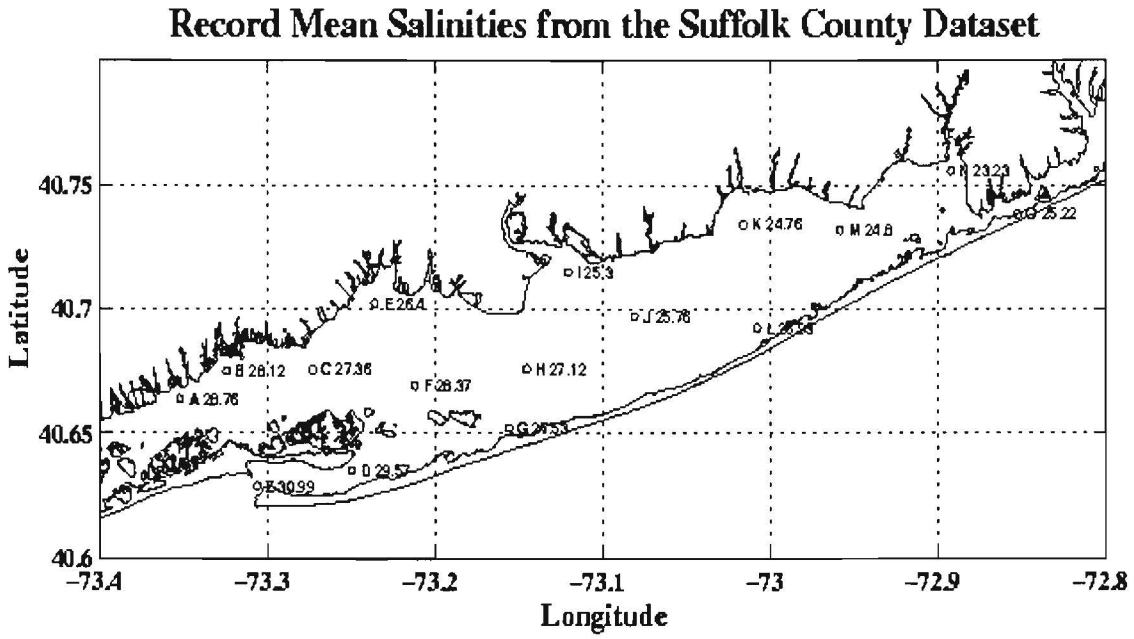

Figure 18. Location of Suffolk County Department of Health Services hydrographic survey stations. Adjacent text includes the station identification letter and the vertically averaged mean salinity value for the all data collected since 1977. Figure supplied by C. N. Flagg, Brookhaven National Laboratory.

It has already been discussed how the salt simulations appear to only approach steady state but were never observed to reach it. Figure 17b represents the change in the model salinity distributions over the last 100 hours (8 individual tidal cycles) of simulation. As can be seen, the results in Moriches Bay and eastern Great South Bay are the most stable with practically no change. The center part of Great South Bay is however apparently increasing in salinity with the western part continuing to decrease. It should be noted that these changes are extremely small, typically less than 0.001 ppt/tidal cycle. Any other process such as periodic flooding or extra-tidal bay flushing, would clearly overwhelm such changes were they to exist in the natural system.

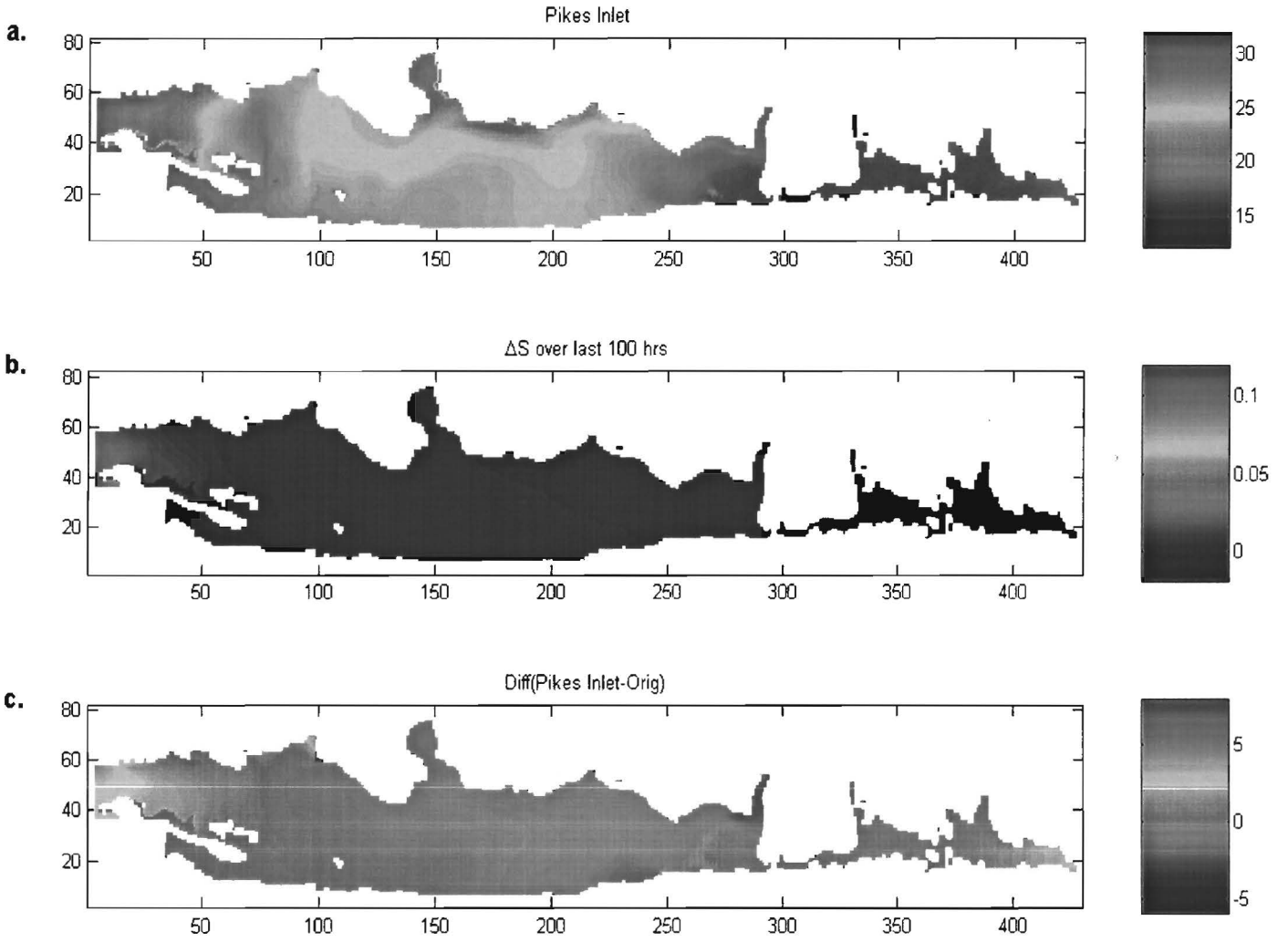

Figure 19. Salinity results for the Pike's Inlet simulation and comparison with the results from the original geometry. Part **a**. shows the bay wide distribution of salinity occurring during slack tide after ebb at Fire Island Inlet, **b**. shows the changes in this value over the final 100 hr. of simulation, and **c**. displays the difference between this simulation and the original. A positive value in c. indicates that this simulation has a higher salinity. Color represents the local value in salinity units and the color bars to right provide the scale. Horizontal and vertical scales are in units of model grid points with 150 m. spacing between grid points.

The results of the salt simulation for Pike's Inlet are shown in Figure 19. In the first part of this figure (Figure 19a) a salinity distribution qualitatively similar to the original simulation (Figure 17a) is seen. Figure 19b indicates that this simulation is approaching steady state with maximum salinity changes smaller than 0.01 ppt/tidal cycle. The region experiencing the most change is the western extremity of the model domain. Figure 19c shows the changes resulting from the simulated breach at little Pike's inlet. In general, the salinity changes associated with this model are very modest with measurable changes occurring only in the eastern end of Moriches Bay and also at the western end of Great South Bay. In both these cases, salinity increased. A slight decrease in salinity is observed throughout much of the rest of Great South Bay, which would suggest a reduced exchange between Great South Bay and Moriches Bay. The mean bay salinity for all of Great South Bay and Moriches Bay decreases slightly from 25.94 ppt for the original geometry to 25.91 ppt for Pike's Inlet. It is not clear why the increase in the west of Great South Bay should occur although increased exchange from Moriches Bay may have freed up a limited amount of Fire Island Inlet flow to feed the western basin.

The predicted changes in salinity for a breach at Old Inlet (Figure 20) or Barret Beach (Figure 21) are considerably larger than those predicted for Pike's Inlet. Figure 20 shows a salinity distribution for Old Inlet in which the salinity of much of Great South Bay has increased on the order of 2-4 ppt. A rather large section of the bay, comprising much of the south-east quadrant appears to have salinities approaching open coast values. The new source of saline water directly into the western basin appears to have nearly erased the fresh water pocket in Nicoll Bay and the strength of the other pocket at the western boundary has been greatly reduced. A very small reduction in salinity is predicted in Moriches Bay where reduced exchange with Great South Bay results in reduced exchange through Moriches Inlet. It is worth noting that the relation between Great South Bay and Moriches Bay regarding salinity has now been reversed so that the former is now the source of the highest salinity water in the system. Overall the mean salinity of the entire system has increased by 3.57 ppt to arrive at a value of 29.51 ppt.
The major differences in the effects on salinity between the Barret Beach breach (Figure 21) and the Old Inlet breach relate to this western end of Great South Bay. Figure 21c indicates that the Barret Beach breach also increases salinity in much of Great South Bay with large areas experiencing a 3-5 ppt increase. The strength of the freshwater tongue at the western boundary is also decreased. However, contrary to the Old Inlet case, the fresh pocket in Nicoll Bay has grown, spreading into northern Patchogue and Bellport Bays. This freshening of the northeast quadrant of the bay (Figure 21c) arises from the shutdown of exchange with Moriches Bay. The presence of Barret Beach breach has paradoxically resulted in an increase in the effective distance between these regions and their source of salt by shutting down the exchange with Moriches Bay. Nonetheless, the mean salinity of the entire system is 28.73 ppt, representing an increase of 2.79 ppt. A slight decrease in the salinity of Moriches Bay is symptomatic of the reduced inter-bay net transport (Figure 9).

DISCUSSION

The model has been shown to provide a relatively good approximation of the tidal response of Great South Bay. Model simulations run with real tide forcing have been shown to reproduce the measured tidal response inside the bay (Figure 5; Table 3). Generic tidal simulations have predicted tidal transmission rates for 5 independent points within Great South Bay with discrepancies of $\leq 3\%$ which in this case is equivalent to a dimensional accuracy of 3.3 cm. Simulations of an observed breach qualitatively predict the observed effects of the breach with slight over prediction of the absolute scale of the effects. The model exhibits some weakness in

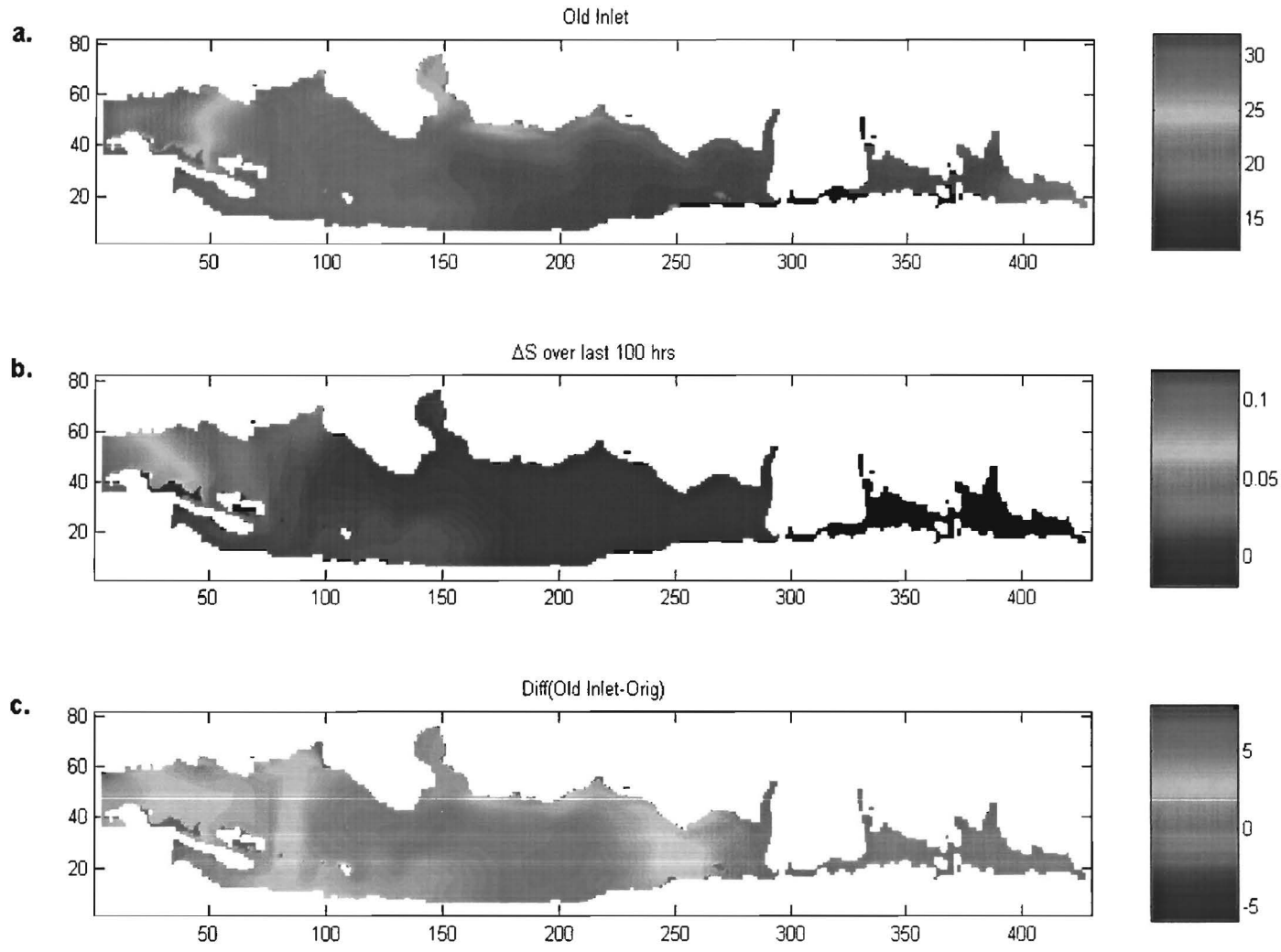

Figure 20. Salinity results for the Old Inlet simulation and comparison with the results from the original geometry. Part **a**. shows the bay wide distribution of salinity occurring during slack tide after ebb at Fire Island Inlet, **b**. shows the changes in this value over the final 100 hr. of simulation, and **c**. displays the difference between this simulation and the original. A positive value in c. indicates that this simulation has a higher salinity. Color represents the local value in salinity units and the color bars to right provide the scale. Horizontal and vertical scales are in units of model grid points with 150 m. spacing between grid points.

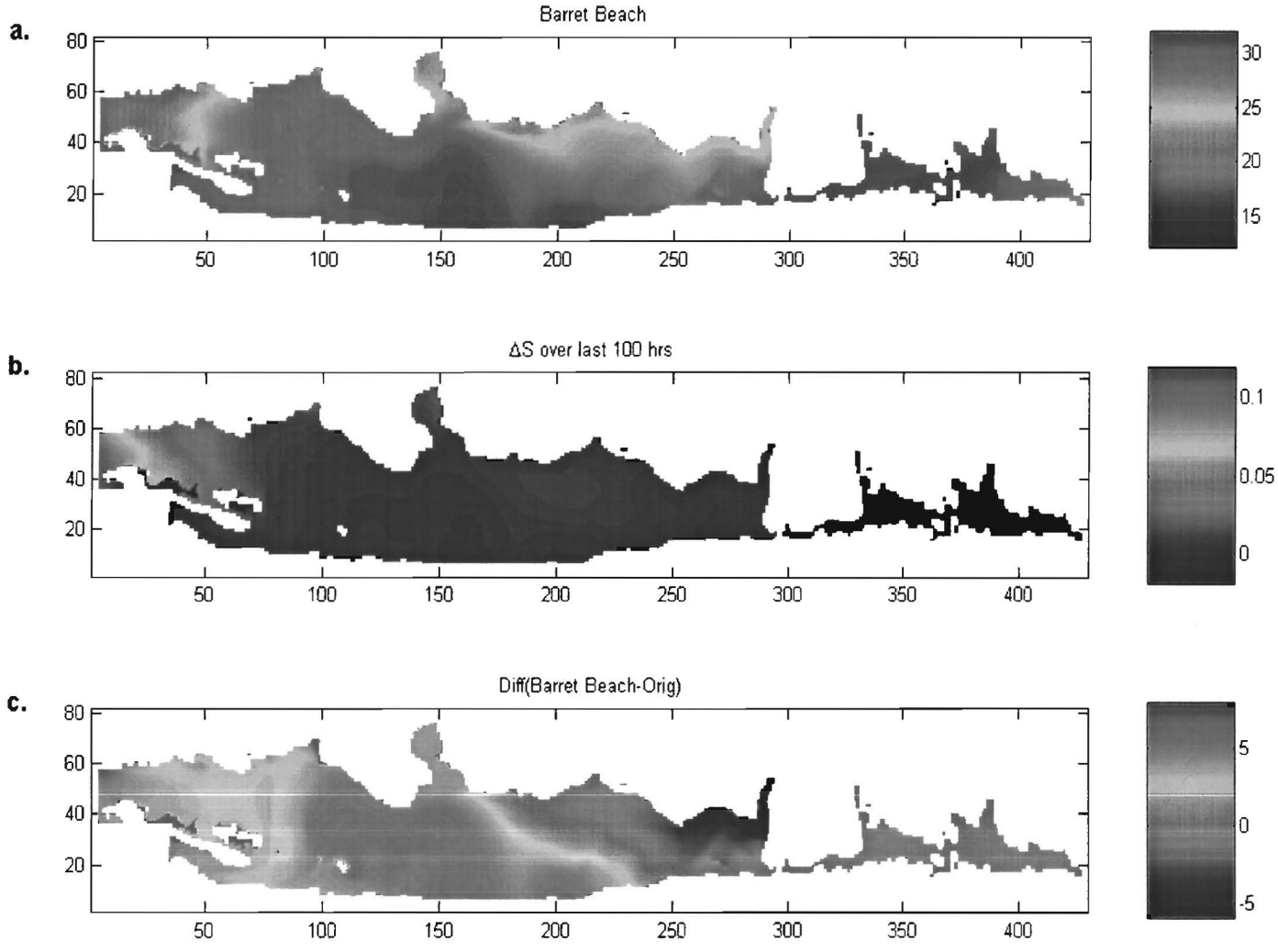

Figure 21. Salinity results for the Barret Beach Inlet simulation and comparison with the results from the original geometry. Part **a**. shows the bay wide distribution of salinity occurring during slack tide after ebb at Fire Island Inlet, **b**. shows the changes in this value over the final 100 hr. of simulation, and **c**. displays the difference between this simulation and the original. A positive value in c. indicates that this simulation has a higher salinity. Color represents the local value in salinity units and the color bars to right provide the scale. Horizontal and vertical scales are in units of model grid points with 150 m. spacing between grid points.

predicting the absolute salinity level in the bay. While the reasons for this weakness have been discussed and in part represent the absence of physical process that may be of great significance in the bay, the result is that the simulations generally under predict salinity. Thus any salinity increases associated with simulated breaches should be considered a worst case scenario. Despite these errors in absolute salinity levels, the simulations have been shown in the case of Little Pike's inlet to predict the salinity changes to within 0.2 ppt, even in regions where the absolute salinity level was poorly predicted. For this reason, we are confident that the model is providing a reasonable estimate of the effects of barrier island breaches on the tidal response of the Great South Bay and Moriches Bay systems.

Pike's Inlet

In general, the simulated effects of a breach at Little Pike's Inlet can be seen to be limited to Moriches Bay. Changes in tidal transmission as well as mean bed stress in Great South Bay are negligible (Figure 10). Salt changes within Great South Bay are small with an increase in salinity to the west and the far east and a decrease in salinity in the near east. This pattern suggests that increased exchange with Moriches Bay (Figure 12) has introduced additional salt near the connection between the two bays. The fresh water from the northeast quadrant of Great South Bay appears to be mixing even less with the intruding Moriches Bay water so that there is a dilution effect to the remaining nearby waters further to the west. Apparently some of the Fire Island Inlet flow which is displaced by the enhanced exchange with Moriches Bay is instead mixing into western Great South Bay leading to an increase in salinity. With the exception of the far west, any changes in salinity are below 1ppt. In Moriches Bay however, the changes are rather dramatic, particularly in the eastern basin. Throughout the entire western basin, tidal transmission increased by over 25%. As reason would dictate, the salinity in this region also rose in parts by more that 2 ppt. Such an increase in tidal transmission has real implications for coastal flooding as regular tidal highs and lows are increased on the order of 15cm. A similar change in storm surges could cause considerable flooding. A 2 ppt change in salinity represents a fairly strong alteration of the estuarine environment and could result in a shift in species structure[e.g. Reid, 1957].

The increase in transmission in the western basin is smaller, typically 5% but as high as 15%. Surprisingly, this higher transmission is not accompanied by an increase in salinity. In fact the salinity in the western basin stays constant in this geometry. This result suggests that the increased salt entering this basin from the ocean is balanced by greater exchange of salt with the southeastern quadrant of Great South Bay. This increased flux between Moriches Bay and Great South Bay is supported by the greater than 30% increase in mean bed scour through the Smith Point narrows (Figure 10). A similar increase in scour is experienced throughout the western basin up to Moriches Inlet. Continuing eastwards, the bed scour is diminished by a similar 30%. This reduction arises due to the new inlet, which provides more direct access to the ocean and accounts for the only major reduction in the 1 dyne/cm^2 sand mobilization threshold in this simulation (Figure 11a). The eastern limit of this threshold recedes approximately 800m in the present simulation. It should be noted that the increases in bed scour described above occur in channels where the peak bed stress is already high. However the reduction in scour occurs over a relatively broad expanse of shallow water in which the reduced peak stress may reasonably be expected to lead to shoaling through the deposition of fine sediments. Similarly the new region of high scour and peak bed stress surrounding the breach would most likely lead to erosion and a transition to coarser grain sizes on the bottom.

The final major change associated with the Pike's Inlet simulation is the development of a large mean transport from the new breach to Moriches Inlet (Figure 9). This mean current is

more efficient at estuarine flushing than simple tidally aided mixing and would no doubt tend to improve water quality throughout central and eastern Moriches Bay for as long as it persists.

Old Inlet

Both the simulated breaches at Old Inlet and Barret Beach have negligible effect on the tidal transmission, circulation, salinity distribution or mean bed stress in Moriches Bay but the effects in Great South Bay are, however, considerably more substantial. A breach at Old Inlet alters the tidal transmission on the order of 4% over an area encompassing greater than 60% of the bay. The great majority of this change is an increase with a small region near the breach experiencing a decrease. Therefore, the scale of tidal transmission effects for such a breach is basin wide but the magnitude of the effect is relatively small. The predicted 4% change in tidal transmission translates to high and low mean tide changes on the order of 2 cm. It seems unlikely that coastal flooding due to regular tides would be a large problem in the advent of such a breach.

Alterations in the estuarine environment due to salinity changes may be a larger problem. The simulations indicate an increase in salinity throughout much of Great South Bay that is of order 3 ppt or greater (Figure 20c). As mentioned earlier, such a change is definitely sufficient to cause shifts in species composition. Paradoxically, the only region not experiencing much of a change is the region around Old Inlet where salinities were already high prior to the breach. It is likely that, had a more realistic simulation of the true freshwater input to this region been utilized, a similar change in salinity would be predicted here. The Old Inlet region may also experience a different environmental change associated with the elevated bed scour. For much of the region around the breach, the bed scour increase approaches 100% with an increase of 20% or greater extending across the bay. These elevated levels occur in a very shallow region with mean depths less than 1 m (Figure 2) and as mentioned earlier are coexistent with a similar area in which peak bed stress exceeds the threshold for sand mobilization (Figure 11b). It is most likely that, should such a breach occur, the region would quickly become incised with channels and that fine sediments would tend to be removed from the region. Much of this fine sediment might be re-deposited in the area in the center of Great South Bay where bed stress levels are seen to decrease up to 60% (Figure 13c) and in which the peak stress has dropped below the mobilization threshold (Figure 11b). A possibly greater environmental effect of such a breach would be the augmented mean transport that develops between the new inlet and Fire Island Inlet (Figure 9). This direct circulation of water from Old Inlet, up along the northern shore of the bay, and out through Fire Island Inlet would clearly tend to improve water quality by greatly decreasing residence time in many parts of the bay. With such a transport, bay-ocean exchange no longer depends solely on dispersion but includes direct advection, which is a much more efficient method of exchange. It is also worth noting that the mean exchange with Moriches Bay is diminished by the presence of this breach, a result which could suggest worsened water quality in Moriches Bay although this could be offset by the proximity to a new source of ocean water.

Barret Beach

While the effects of a breach at Barret Beach share many similarities with those resulting from a Pike's Inlet Breach, there are also some significant differences. As this breach provides a new inlet at the center of the bay, changes in tidal transmission are relatively uniform with an increase occurring throughout Great South Bay (Figure 15a). A slightly higher increase ($\approx 4\%$) to the west serves to smooth out bay wide variations in transmission. However, as in the case of Old Inlet, the increase in tidal transmission due to a breach at Barret Beach is equivalent to a

change in tide levels on the order of 2 cm and is likely to cause relatively little trouble related to flooding. The breach does result in very pronounced changes in salinity in Great South Bay with generally increasing salinity in the west and decreasing salinity in the east. The 3-6 ppt increase in salinity in the western two thirds of the bay is symptomatic of increased exchange with the ocean and suggests lower residence time and increased water quality in this area. Much of the increase is probably associated to a pronounced strengthening of the direct transport from the center of the bay out through Fire Island Inlet (Figure 9). The level of salinity increase produced by these changes will undoubtedly result in a species composition shift towards more oceanic species. The up to 4 ppt decrease in salinity in the eastern third indicates reduced mixing with ocean waters largely because of an apparent weakening of the tidal exchange and the advection from Moriches Bay. These changes similarly suggest an increase in the residence time and a decrease in water quality for this section at the same time that the rest of the bay is experiencing improved water quality. Again, as in the case of the Old Inlet breach, reduced bed stress near the center of the bay (Figure 11c) will likely result in a shift in bottom sediment type. Unlike the Old Inlet case, the enhanced bed stress near the new breach is localized so that the sand mobilization threshold is exceeded only in a narrow strip approximately 2 km long and 0.3 km wide surrounding the new breach (Figure 11c).

Table 5

Residence times (T_R) in days calculated from model simulations using (3). Residence times for different bays are calculated by applying (3) only to the respective region of the model domain.

	Original Geometry	*Pikes Inlet*	*Old Inlet*	*Barret Beach*
Total Bay T_R	96.3	96.7	39.51	51.9
Great South Bay T_R	100.2	101.1	40.3	53.3
Moriches Bay T_R	23.9	13.6	25.8	27.0

Residence Time

The "residence time" of an estuary is a global parameter intended to represent the time, on average, that a parcel of water will remain within the estuary. This quantity is often calculated based on the flood tidal volume and the volume of water in the bay. The problem with such a formulation is that it tends to neglect the fact that a variable fraction of the flood tidal volume represents actual new sea water, thereby grossly underestimating the effective residence time. A more representative approach is to calculate the residence time based on the freshwater input [Fischer et al.,1979] which is always of new origin. The equation for this residence time, T_R, is:

$$T_R = \frac{\oint_{Bay} f\,dv}{Q_{fresh}} \qquad (3$$

Where the integral is taken over the bay volume, Q_{fresh} is the freshwater flux rate, and $f = (S_O - S)/S_O$ is the "freshness" parameter which is 1 when the water is fresh ($S=0$) and 0 when the water is pure sea water ($S=S_O$). Table 5 gives various residence times in days for the different simulations. It is clear that the two breach geometries that have the greatest impact on the global residence time are Old Inlet and Barret Beach with Old Inlet reducing the residence

time by almost 2/3^{rds}. While the Pike's Inlet breach had little effect on the system as a whole, it halved the residence time for Moriches Bay while the other 2 breaches slightly increased it.

Storm Surges and Flooding

The transmission of storm induced changes in sea level into an estuary is comparable to tidal transmission but there are 3 additional factors that must be considered, the time scale of the storm driven effects, the geometry of the inlet, and the nature of the land topography surrounding the estuary. The time scale is very important because the inlet only acts as a filter on tidal transmission with the level of transmission being strongly dependent on the duration of the sea surface anomaly. Thus a tide or storm surge of "infinite" period (e.g. eustatic sea level change) will eventually be transmitted in it's entirety and an instantaneous change (e.g. tsunami) would have effectively no transmission (through the inlets at least). Inlet geometry is of interest because as sea level rises, more and more of the inlet surroundings will be flooded effectively increasing the inlet cross-sectional area and enhancing the transmission of the elevated sea level. With the opposite effect is the fact that as the water in the bay rises, the surrounding land is flooded and the effective bay area increases. If the land surrounding the bay is low lying marsh land, this effect can be pronounced, effectively curtailing sea level transmission.

When we consider the transmission of semi-diurnal tides into Great South Bay, the bay is on average spending 6 hours filling. Over those 6 hours, the inlets pass the equivalent of 30% of the tidal range. Thus, as an approximation, it is reasonable to assume that any storm surge on the order of 1 m, which is present for 24 hours, will be passed to the bay in its entirety. While the second and third arguments in the preceding paragraph have not been considered in this discussion, their combined effect along with the margin of error provided for in the 24 hour limit render it still valid. As most extra-tropical storms are typically of that length or greater, inlet transmission is probably only a consideration for faster traveling shorter period storms such as hurricanes. For such storms in which 12 hours is a reasonable approximation of the period of the storm, the results of the tidal transmission simulations are transferable to the storm surge. Namely, in the case of breaches at Barret Beach and Old Inlet, the transmission of the storm surge would on average be on the order of 5% more than it would be without the breaches.

Temperature

The temperature of the water in an estuary is a non-conservative property that is controlled not only by the original temperature of mixing water masses but also by flow of heat through surrounding surfaces. On the contrary, for this model, salt is treated as a conservative property with which basic bookkeeping (how much salt flows in and how much flows out) is required to determine the salinity of the water. It is assumed that there are no processes other than transport and eddy diffusion that can change the amount of salt in the water. As evaporation and salt storage in sediments are relatively low in Great South Bay, this is a reasonable approximation. The qualitative results obtained for salinity may be applied to understand the effects of breaches on other water properties as long as the ocean and/or groundwater act as sources for that property and it can be reasonably approximated as a conservative quantity. Absolute values may however differ due to differences in the magnitude of the respective horizontal mixing coefficients. The problem with other state variables for this system such as temperature or oxygen is that they are non-conservative. While this model is perfectly capable of keeping track of the transport of these quantities, it is not capable of determining local heating and cooling of the water nor respiration and decomposition, processes which may have as much to do with the local concentration of

temperature and oxygen as transport processes. For this reason, simulation of the effect of breaches on these quantities was beyond the scope of this project.

Inlet Stability

The traditional engineering definition of inlet stability defines a stable inlet as one in which a reduction in the inlets cross section will result in an increase in the maximum inlet velocity and an increase in cross section will lead to a reduction in maximum velocity [Keulegan, 1967]. The assumption behind this definition is that such changes in velocity would lead to erosion or deposition as required to return the inlet to it's original geometry. A complete traditional inlet stability analysis would require running a series of simulations in which the inlet cross section is varied. Stability would then require that a region of inlet stability was found to exist simultaneously among all the inlets in the system. A final step, which relates to each local condition, is to determine whether this stable region is strong enough to keep the inlet clear of all the sediment delivered to the inlet by the littoral drift. This analysis was also beyond the scope of this project. It is however possible to look at the bed stress results for the simulations and conjecture about the likelihood of such a breach remaining open.

Considering the flow that develops in the Pike's Inlet simulation, we see that currents generated are as large or larger than those in neighboring Moriches Inlet (Figure 12). Looking at the stress changes we see that the enhanced stress does cover much of the width of the bay in this location (Figure 10c) but we also see that the area covered by this pattern appears to be less than the area of the approaches to Moriches Inlet. For these reasons, it appears reasonable to suggest that should a breach occur at Little Pike's Inlet and arrive at the size simulated in these tests, that inlet would have a good chance of remaining open. A similar breach at Old Inlet appears to be less likely to remain open. In such a breach, the currents generated appear to be somewhat weaker than those in Fire Island Inlet suggesting a weaker ability to clear the inlet (Figure 14). Additionally, the location of this breach is a very shallow section of the bay (Figure 2) where currents apparently have to traverse the bay to arrive at reasonable conveyance channels. This results in a very large region of greatly enhanced bed stress that would tend to resist the development of such an inlet. Finally, the fairly strong flood tide asymmetry apparent in Figure 14 suggests that sediment from the new breach would be carried into the bay side of the breach. While the removal of this sediment from the littoral circulation might generally be considered favorable to inlet growth, it may have the effect to fatally choke the immature inlet in this shallow environment. The apparent flood tide dominance of the Barret Beach breach (Figure 16) would in fact be looked on favorably as in this deeper, more open location, this dominance would tend to remove sediment from where it could be reworked by waves to close the inlet. The bed stress pattern (Figure 15) shows elevated bed stress levels local to the inlet only with flow that is free to diverge and converge at the inlet throat (Figure 16). Tidal currents through the breach appear to be as great or greater than those in Fire Island Inlet. Thus it appears that a breach occurring in this location has a good chance of persisting once it attains the dimensions simulated in the model.

Extra Tidal Storm Induced Motions

One of the more critical shortcomings of the present model is failure to address long period, extra-tidal circulation in the model. Several investigators have discussed the importance of non-tidal forcing of circulation in Great South Bay and Moriches Bay [Wong and Wilson, 1985; Wilson et. al., 1991]. This type of forcing can occur in two forms, the first involves storm surge and coastal setup and setdown where a regional change in the mean sea surface elevation will tend to drive circulation into or out of both (all) inlets simultaneously similarly to regular tidal

forcing. The second type of forcing involves direct, along bay axis, wind forcing which will tend to set up water towards the downwind end of the bay. This type of forcing drives a direct current in through the upwind inlet(s) and out through the downwind inlet(s). While the former relies on horizontal and vertical mixing to transmit salt etc. into the bay, the latter involves direct water replacement and is a more efficient mechanism for the exchange of salt. Figure 22 highlights a 9 day period of time near the beginning of the second deployment. Starting around midnight on the 4th of April 1995, a large salinity jump is seen to occur simultaneously across the bay with changes in salinity of greater than 3 ppt occurring over 2 days. During this same period of time the mean water level in the bay drops on the order of 40 cm. The drop is seen to occur concurrently with the appearance of strong northwesterly winds, which are favorable for causing a setdown of the coastal sea surface, as well as to drive an west-east current along the axis of the bay system. The importance of such an event can be understood by the fact that it took the model over half a year of simulated time to approach equilibrium where the largest salinity change was also of order 4 ppt! Whether or not the presence of the simulated breaches increases or decreases the strength of these episodes of direct exchange may have as much to do with their effects on the salinity and water quality of the bay as the tidal mixing examined in this study.

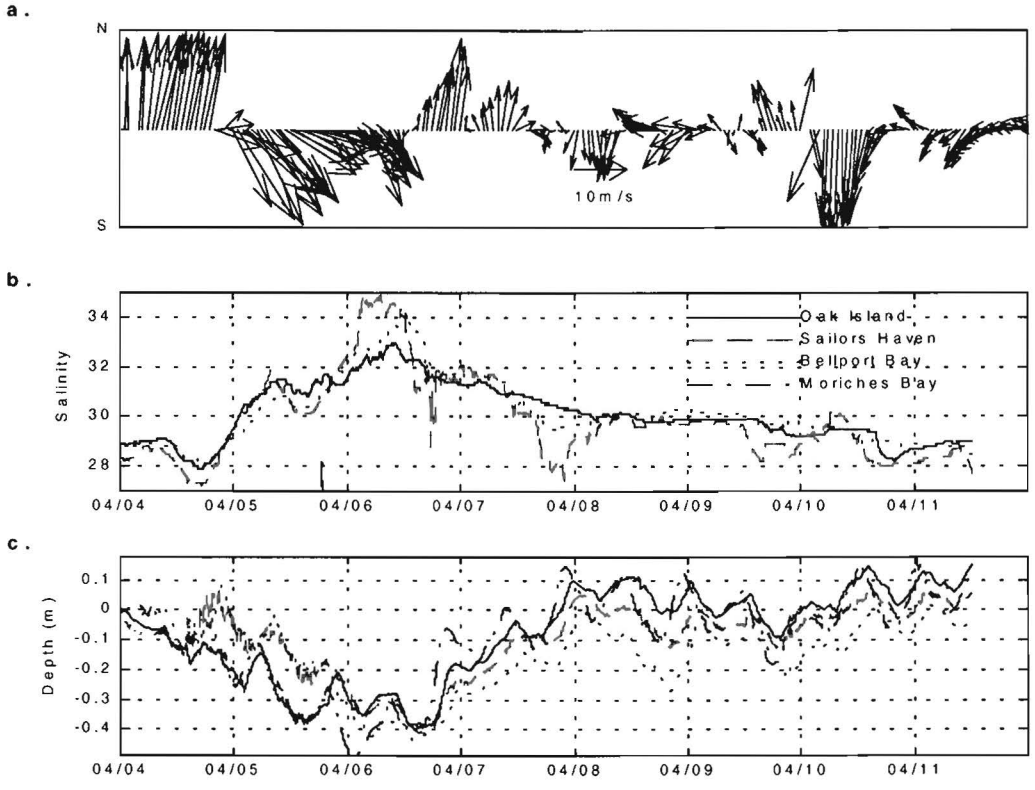

Figure 22. Detailed plot of salinity change event seen in figures 3 and 4. Figure displays (**a**.) wind velocity vectors (from NOAA data buoy Long Island #44025), (**b**.) salinity data and (**c**.) relative depth for the four functioning measurement stations. Wind vectors indicate mean direction and velocity and are plotted hourly. Wind blowing towards the north would be plotted as a vector pointing up. Moriches conductivity sensor was not working at this time but the temperature sensor shows an analogous drop corresponding to this period.

It is also possible that tidal flooding is also dependent on this type of internal bay setup where strong along-axis winds mass water at one end of the bay or the other. The effect of barrier island breaching on flooding of this type may be exactly the opposite of that associated with tides and storm surge. Using the example of Little Pike's Inlet, it has been shown how the presence of this breach increases the transmission of tides (and would similarly increase the transmission of storm surge). However, in the case of intra-bay setup, this breach might actually reduce flooding by providing an extra "safety valve" for draining off elevated water levels. Further study on the effects of such breaches must investigate the importance of regional storm surge vs. local setup to bay flooding as well as determining how the presence of additional inlets would affect these phenomena.

CONCLUSIONS

The model has been shown to reliably predict tidal elevation changes in Great South Bay for both present conditions as well as for cases with additional inlets. The salinity predictions are not completely accurate in magnitude but tests involving Little Pike's Inlet suggest that the changes in salinity are well predicted with the model results suggesting a worst case scenario.

The simulations indicate that the effects of a breach at Little Pike's Inlet in Moriches Bay would be predominantly felt in that Bay. The changes in tidal transmission for this case are the largest for any of the simulations performed with tidal transmission increased by 15-30% over much of Moriches Bay. The presence of the inlet leads to a small net circulation through Moriches Bay. Salinity changes are relatively modest with a 1-2 ppt increase experienced in the eastern half of Moriches Bay. While the model predicts similar changes in the west of Great South Bay, it is felt that these are artifacts of the simulation boundary conditions. Global residence time for the system is relatively unchanged but the residence time for Moriches Bay is reduced from 23.9 to 13.6 days.

Changes in tidal transmission for simulated breaches at Old Inlet and Barret Beach are relatively modest, with the largest change in transmission on the order of 4%. Both simulations result in a reasonably strong mean current generation within the bay which would most likely decrease the mean residence time within most parts of Great South Bay and lead to an improvement in water quality. This is especially true for the simulated breach at Old Inlet where this net circulation traverses most of the Bay and drains a region of the bay that is presently fairly stagnant. Computed global residence times for the system were 39.5 and 51.9 days respectively as compared to 96.3 days for the original geometry.

Salinity changes for both of these simulated breaches are significant. A breach at Old Inlet will raise the mean salinity of the entire system from 25.9 ppt to 29.5 ppt with this increase spread relatively evenly across Great South Bay. Weaknesses in the model freshwater input scheme would probably mean that the changes in salinity in Bellport Bay are severely understated in this case. Similarly large salinity changes are predicted for much of Great South Bay with a breach at Barret Beach. The mean bay salinity is increased to only 28.7 ppt because a significant freshening is predicted for Bellport Bay.

Peripheral evidence argues that a breach at Old Inlet would be the least likely to remain open while a breach at Barret Beach may in fact be the most likely. A follow up study designed is required to determine just what inlet stability for inlets derived from these breaches might be as well as to determine the equilibrium size for such an inlet.

There is strong suggestion that secondary extra-tidal effects may be extremely important in determining the flooding potential and water quality effects of a new inlet in Great South Bay. Additional study is needed into what the role of these effects on water quality and coastal flooding are and how additional inlets might alter these effects.

REFERENCES

Chant, R.J. *Tidal dynamics of the Hudson River Estuary*, Ph.D. dissertation, Marine Sciences Research Center, State University of New York, Stony Brook. 1995.

Conley, D.C. Observations on the impact of a developing inlet in a bar built estuary. *Continental Shelf Research*, 19, 1733-1754, 1999.

DiLorenzo, J.L. The overtide and filtering response of small inlet/bay systems. in *Hydrodynamics and Sediment Dynamics of Tidal Inlets.* edited by D.G. Aubrey and L. Weishar, pp. 24-53, Springer-Verlag, New York, 1988.

Fischer, H.B., E.J. List, R.C.Y. Koh, J. Imberger, and N. Brooks, *Mixing in inland and coastal waters.* pp. 1-483, Academic Press, San Diego, 1979.

Giese, G.S. Cyclical behavior of the tidal inlet at Nauset Beach, Chatham, Massachusetts. in *Hydrodynamics and Sediment Dynamics of Tidal Inlets.* edited by D.G. Aubrey and L. Weishar, pp. 269-283, Springer-Verlag, New York, 1988.

Keulegan, G.H. Tidal flow in entrances. Water-level fluctuations of basins in communication with seas. *Technical Bulletin,* No. *14*, pp. 1-89, U. S. Army Corps of Engineers, 1967.

Koutitonsky, V.G., R.E. Wilson, D.S. Ullman, and C. Toro, "SWK3D: An enhanced version of the VANERN three-dimensional hydrodynamical model for applications to stratified semi-enclosed seas. *Contract Rep. FP 707-6-5361,* pp. 1-110, Inst. Natl. de la Rech. Sci. Oceanol. 1987.

Leatherman, S.P. Role of the inlet in the geomorphic evolution of the south shore barriers of Long Island. *Environmental Management, 13*, 109-115, 1989.

Mehta, A.J. and P.B. Joshi, Tidal inlet hydraulics. *Journal of Hydraulic Engineering, 114*, 1321-1338, 1988.

Pritchard, D.W. and E. Gomez-Reyes, A study of the effects of inlet dimensions on salinity distributions in Great South Bay: Final Report. No. *86-7*, pp. 1-64, Marine Sciences Research Center, 1986.

Pugh, D.T. *Tides, surges, and mean sea-level.* -1-472, J. Wiley, Chichester, 1987.

Redfield, A.C. Report to the Towns of Brookhaven and Islip, N.Y., on the hydrography of Great South Bay and Moriches Bay. No. *52-26*, pp. 1-80, Woods Hole Oceanographic Institution, 1952.

Reid, G.K. Biologic and hydrographic adjustment in a disturbed Gulf Coast estuary. *Limnol. Oceanogr. 2*, 198-212, 1957.

Turner, E.J. Effects of a storm-induced breach on Mercenaria mercenaria in Moriches Bay. Masters thesis, Marine Sciences Research Center, State University of New York, Stony Brook 1-77, 1983.

Ullman, D.S. and R.E. Wilson, Model parameter estimation from data assimilation modeling: Temporal and spatial variability of the bottom drag coefficient. *Journal of Geophysical Research, 103*, 5531-5549, 1998.

Valle-Levinson, A. and R.E. Wilson, Effects of sill bathymetry, oscillating barotropic forcing and vertical mixing on estuary ocean exchange. *Journal of Geophysical Research, 99*, 5149-5169, 1994.

van de Kreeke, J. Hydrodynamics of tidal inlets. in *Hydrodynamics and Sediment Dynamics of Tidal Inlets*. edited by D.G. Aubrey and L. Weishar, pp. 1-23, Springer-Verlag, New York, 1988.

Wessel, P. and W.H.F. Smith, Free software helps map and display data. *EOS, Transactions, American Geophysical Union, 72*, 441 1991.

Wessel, P. and W.H.F. Smith, New version of the Generic Mapping Tools released. *EOS, Transactions, American Geophysical Union, 76*, 329 1995.

Wilson, R.E., K. Wong, and H.H. Carter, Aspects of circulation and exchange in Great South Bay. in *The Great South Bay*. edited by J.R. Schubel, T.M. Bell, and H.H. Carter, pp. 9-21, State University of New York Press, Albany, 1991.

Wong, K. and R.E. Wilson, Observations of low-frequency variability in Great South Bay and relations to atmospheric forcing. *Journal of Physical Oceanography, 14*, 1893-1900, 1985.

Wong, K. *Subtidal volume exchange and the relationship to atmospheric forcing in Great South Bay*, Ph.D. dissertation, Marine Sciences Research Center, State University of New York, Stony Brook.1-230, 1981.